Accepted to AJ
Preprint typeset using LaTeX style emulateapj v. 5/2/11

ROBO-AO KEPLER PLANETARY CANDIDATE SURVEY II: ADAPTIVE OPTICS IMAGING OF 969 KEPLER EXOPLANET CANDIDATE HOST STARS

Christoph Baranec[1], Carl Ziegler[2], Nicholas M. Law[2], Tim Morton[4], Reed Riddle[3], Dani Atkinson[1], Jessica Schonhut[1, 5] and Justin Crepp[6]

Accepted to AJ

ABSTRACT

We initiated the Robo-AO *Kepler* Planetary Candidate Survey in 2012 to observe each *Kepler* exoplanet candidate host star with high-angular-resolution visible-light laser-adaptive-optics imaging. Our goal is to find nearby stars lying in *Kepler*'s photometric apertures that are responsible for the relatively high probability of false-positive exoplanet detections and that cause underestimates of the size of transit radii. Our comprehensive survey will also shed light on the effects of stellar multiplicity on exoplanet properties and will identify rare exoplanetary architectures. In this second part of our ongoing survey, we observed an additional 969 *Kepler* planet candidate hosts and we report blended stellar companions up to $\Delta m \approx 6$ that contribute to *Kepler*'s measured light curves. We found 203 companions within $\sim 4''$of 181 of the *Kepler* stars, of which 141 are new discoveries. We measure the nearby-star probability for this sample of *Kepler* planet candidate host stars to be 10.6% ± 1.1% at angular separations up to $2''.5$, significantly higher than the 7.4% ± 1.0% probability discovered in our initial sample of 715 stars; we find the probability increases to 17.6% ± 1.5% out to a separation of $4''.0$. The median position of KOIs observed in this survey are 1.1° closer to the galactic plane which may account for some of the nearby-star probability enhancement. We additionally detail 50 Keck adaptive optics images of Robo-AO observed KOIs in order to confirm 37 companions detected at a $< 5\sigma$ significance level and to obtain additional infrared photometry on higher-significance detected companions.

Subject headings: binaries (including multiple): close - instrumentation: adaptive optics - instrumentation: high angular resolution - planetary systems - planets and satellites: detection - planets and satellites: fundamental parameters

1. INTRODUCTION

The primary *Kepler* mission photometrically observed approximately 200,000 stars for 4 years in the search for transiting exoplanets. As of the Q1-Q17 DR24 dataset release (Coughlin et al. 2015), there are 3,324 *Kepler* Objects of Interest (KOI) stars in the *Kepler* input catalog that are designated as either 'CONFIRMED' or 'CANDIDATE' in the NASA Exoplanet Archive (Akeson et al. 2013), with 4,302 repeating transit signals indicative of transiting exoplanets. While *Kepler* is one of the best facilities to measure the periodic dips in stellar brightness caused by transiting exoplanets, it has a coarse pixel size, $\sim 4''$, and a mean 95% encircled-energy diameter of 4.3 pixels (Haas et al. 2010) that make it unsuitable for reliably detecting multiple sources within the *Kepler* photometric apertures. Follow-up high-angular-resolution imaging of KOIs is used to determine the sources contributing to the *Kepler* light curves in order to rule out astrophysical false positives (e.g., Morton & Johnson 2011, Dressing & Charbonneau 2013, Fressin et al. 2013, Santerne et al. 2013), to accurately measure the radii of the detected planets with respect to their host star (e.g., Campante et al. 2015; Ciardi et al. 2015), to measure the effect of stellar multiplicity on exoplanet formation (e.g., Wang et al. 2014b,a, 2015b,a), and to study other astrophysical phenomena (e.g., Muirhead et al. 2013; Montet et al. 2015).

In 2012, we initiated the Robo-AO *Kepler* Planetary Candidate Survey in an effort to systematically observe each *Kepler* planet candidate host star in a consistent way with adaptive optics (AO). No AO survey of this magnitude had previously been attempted and this type of survey has only recently been made possible with the commissioning of the Robo-AO robotic laser adaptive optics system that can observe more than 200 objects in a single night (Baranec et al. 2014b). We expect that the results of this survey will be used in validating candidate exoplanets, correcting the estimates of transit radii, identifying rare and interesting exoplanetary system architectures and exploring the properties and trends of exoplanets in multiple star systems.

During our first observing season in 2012, we observed 715 KOIs with Robo-AO (Law et al. 2014, henceforth Paper I). Of the 715 KOIs observed, we found 53 to have a fainter stellar companion within a $2''.5$ radius, leading to a nearby-star probability of 7.4% ± 1.0%. We now report results from the second part of our ongoing survey, comprising a further 969 observations of KOIs with Robo-AO. We additionally report Keck adaptive optics

baranec@hawaii.edu
[1] Institute for Astronomy, University of Hawai'i at Mānoa, Hilo, HI 96720-2700, USA
[2] Department of Physics and Astronomy, University of North Carolina at Chapel Hill, Chapel Hill, NC 27599-3255, USA
[3] Department of Astrophysical Sciences, Princeton University, Princeton, NJ 08544, USA
[4] Division of Physics, Mathematics, and Astronomy, California Institute of Technology, Pasadena, CA 91125, USA
[5] University of Hertfordshire, Hatfield, Hertfordshire AL10 9AB, United Kingdom
[6] Department of Physics, University of Notre Dame, Notre Dame, IN 46556, USA

images of 50 of the Robo-AO observed KOIs to confirm companion detections made at low significance, $< 5\sigma$, and to obtain additional infrared photometry that will later be used to better constrain photometric parallaxes to determine if the companions are physically associated (D. Atkinson et al., 2016, in preparation). Of the 969 KOIs observed, we have found 203 companions[7] of which 141 are new discoveries.

This paper is organized as follows. In Section 2 we describe the KOI survey target selection and the observations made with Robo-AO and NIRC2. Sections 3 and 4 describe the Robo-AO and NIRC2 data reduction and companion-detection pipelines respectively. In Section 5 we describe the results of the survey, including the discovered companions, and compare these with other surveys and observations. In Section 6 we discuss implications of the survey and how others can use these observations. Finally, we conclude with plans for current and future work in Section 7.

2. SURVEY, TARGETS AND OBSERVATIONS

2.1. *Target Selection*

We selected targets that we had not previously observed from the KOIs Catalog based on the Q1-Q12 *Kepler* data (Rowe et al. 2015). These targets were added to the Robo-AO intelligent observing queue (Riddle et al. 2014) and observed during the summer of 2013. While we imposed no artificial magnitude limit on the targets, there were only 4 targets fainter than 16th magnitude that we effectively observed. In Figure 1 we compare the Robo-AO imaged KOIs to the distribution of all current KOIs (Coughlin et al. 2015). The four graphs show the comparisons in the characteristics of KOI stellar magnitude and effective temperature; and planetary orbital period and radius. The list we have observed correlates closely with the *Kepler* Q1-Q17 DR24 list in all of these categories, with the exception of the longest period planets which are fewer in number in the Q1-Q12 list due to the shorter time baseline. It is only by coincidence that we did not observe the small number of KOIs with 15 - 20 $R_\oplus$ companions nor with stellar temperatures higher than 8000 K.

2.2. *Observations*

2.2.1. *Robo-AO*

We obtained high-angular-resolution images of 956 *Kepler* planet candidate host stars over the course of 19 nights between 2013 July 21 and 2013 October 25 detailed in Table 5 in the Appendix. We also include 13 images from 2012 that required additional confirmation of the KOI position in the Robo-AO field of view. All the observations were performed in a queue-scheduled mode in combination with other science programs using the Robo-AO autonomous laser adaptive optics system (Baranec et al. 2013, 2014b) mounted on the robotic 1.5-m telescope at Palomar Observatory (Cenko et al. 2006). Table 1 summarizes the system and survey specifications.

Each observation comprises a sequence of full-frame-transfer detector readouts of an electron multiplying CCD camera at the maximum rate of 8.6 Hz. Individual frames are later registered to correct for the dynamic image displacement of the KOI (Section 3) that cannot be measured with the laser guide star. A total exposure integration time of 90 seconds was chosen so that close sources up to roughly 6 magnitudes fainter than the *Kepler* object would be detected. For the majority of these observations a long-pass filter with a cut-on wavelength of 600 nm was used (LP600 hereafter). The LP600 filter approximately matches the *Kepler* passband at the redder wavelengths whilst simultaneously suppressing the blue wavelengths. The blue wavelengths will degrade adaptive optics performance in the majority of seeing conditions. Compared to near infrared adaptive optics observations, the LP600 filter more closely approximates the direct measurement of the effects of any unresolved companions for the relevant *Kepler* light curves. An i'-band filter (York et al. 2000) was used during eight of the 2012 observations in an attempt to obtain slightly sharper images of brighter targets. A comparison of the two filters can be found in Paper I.

There are two main factors that affect the quality of images acquired by Robo-AO: atmospheric seeing and the brightness of the target. For bright targets ($m_V < 13$), in median seeing of $1\farcs1$ (Cenko et al. 2006), Robo-AO can obtain images with a Strehl ratio of 9%, and full-width at half-maximum (FWHM) of $0\farcs12$ in i'-band. As the seeing approaches $1\farcs6$, the Strehl ratio drops to 5%. For fainter targets, i.e. $m_V > 14$, there needs to be a sufficient number of photons in the diffraction limited core captured during each frame-transfer exposure for post-facto image registration techniques to maintain full acuity. Robo-AO is able to capture scientifically useful images on these fainter targets during times when the atmospheric seeing is favorable, so observations are often repeated until data of sufficient quality is obtained. We adopted the same automated routines used by Paper I to measure the actual imaging performance and to classify the targets into the imaging performance classes given in the full observations list; this classification was used with the contrast curve for each class to estimate the companion-detection performance for each target (Section 3.5).

2.2.2. *Keck adaptive optics*

We obtained images of 50 KOIs with the NIRC2 instrument behind the Keck II adaptive optics system that were previously observed with Robo-AO and had evidence of a companion. For KOIs brighter than $m_V \sim 13$ we typically used the KOI as the guide star in natural-guide-star mode, and for fainter KOIs we used the laser guide star, using the KOI as the tip-tilt-focus guide star (Wizinowich et al. 2006; van Dam et al. 2006). Observations were conducted on 2013 June 25, 2013 August 24 and 25, 2014 August 17 and 2015 July 25 in the K, Ks or Kp filters, and in the narrow mode of NIRC2 (9.952 mas pixel^{-1}; Yelda et al. 2010). An initial 30 s exposure was taken for each target, and we waited for the low-bandwidth wavefront sensor to settle if the laser was used. The integration time and number of coadds per detector readout were adjusted to keep the peak of the stellar PSF counts less than 8,000 ADU per single integration (roughly half the dynamic range where sensitivity of the detector is linear), while maintaining a total ex-

[7] For brevity we denote stars which we have found within our detection radius of KOIs as "companions," in the sense that they are asterisms associated on the sky.

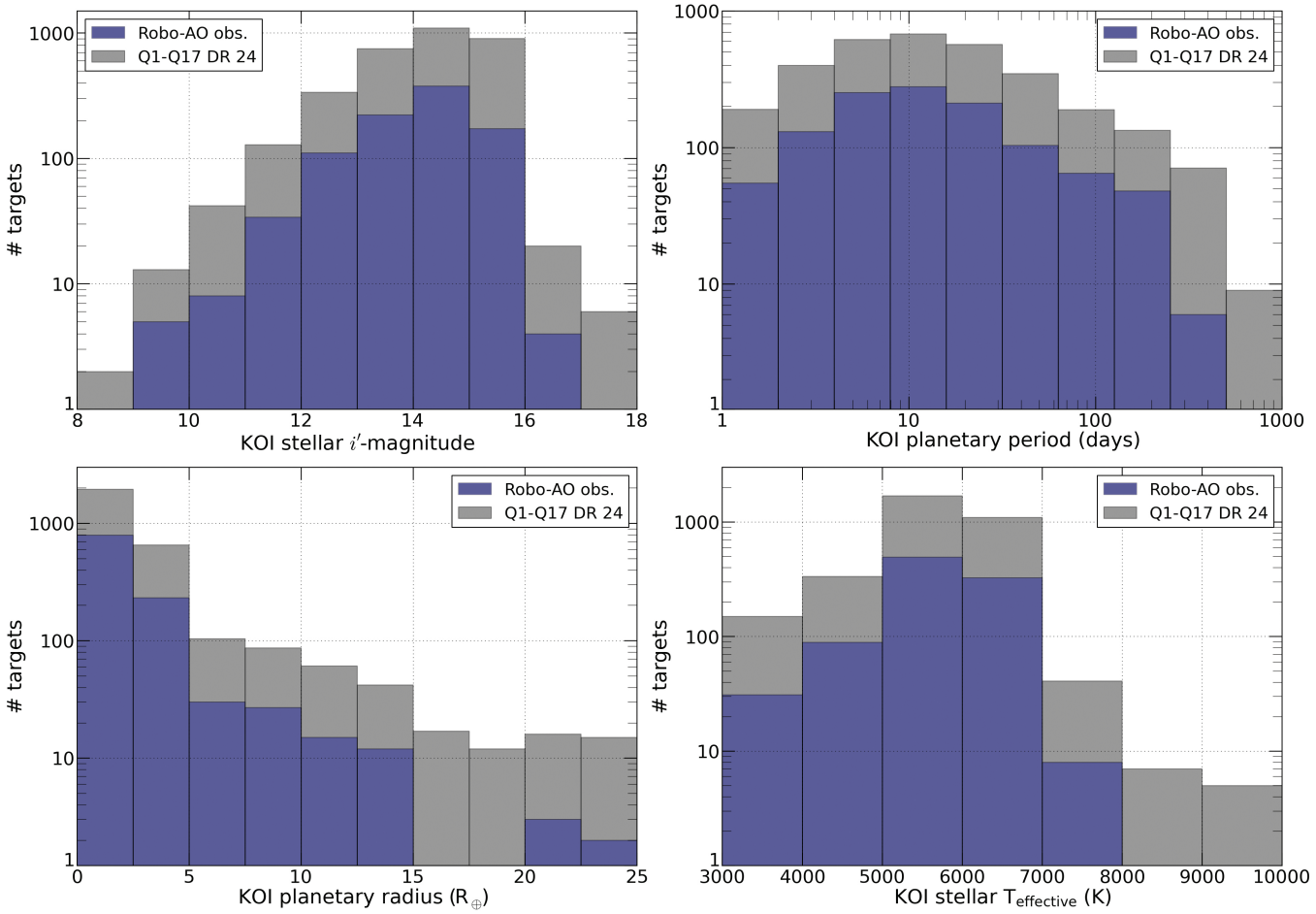

Figure 1. Comparison of the distribution of the Robo-AO sample in this paper, from Q1-Q12 (Rowe et al. 2015), to the set of KOIs from Q1-Q17 DR 24 (Coughlin et al. 2015).

Table 1 Specifications of the Robo-AO KOI survey

KOI targets	969
Exposure time	90 seconds
Observation wavelengths	600–950 nm
FWHM resolution	0.″12–0.″15
Field of view	44″× 44″
Pixel scale	43.1 mas / pix
Detector format	1024^2 pixels
Observation dates	2012 July 16 – 2012 September 13
	2013 July 21 – 2013 October 25
Targets observed / hour	20

posure time of 30 s. Dithered images were then acquired with the primary centered in the 3 lowest noise quadrants using the 'bxy3 2.5' command, for a total exposure time of 90 s.

3. ROBO-AO DATA REDUCTION

We adopted the same automated data reduction and analysis pipeline used in Paper I and we briefly review it here, along with minor improvements. We first manually find the location of the KOI in the field using a preliminary reduction of the data (Section 3.1). The pipeline first takes the short-exposure data cubes recorded by the electron multiplying CCD camera and produces dark, flat-field and tip-tilt-corrected co-added output images (Section 3.2). We then subtract a locally optimized point-spread function (PSF) estimate from the image of the Kepler target in each field (Section 3.3), and either detect companions around the target stars or place limits on their existence (Section 3.4). Finally, we measure the properties of the detected companions (Section 3.6).

3.1. *Target Confirmation*

We manually checked the location of the KOI in Digital Sky Survey (DSS) images and selected the KOI itself as the guide star to correct image displacement in each observation. In this survey, for fields where the DSS image was insufficient for KOI identification, or if the proper motion of stars made the target ambiguous, we would use the publicly available recent UKIRT J-band images of the Kepler field. For a minority of targets, there was only a single star in the field of view. For these targets, we first confirmed with UKIRT images that there were no other sources within our field; then we confirmed whether the telescope pointing offsets were stable for that particular observation by noting if prior and subsequent KOI targets landed in the same area of the detector. We note that Paper I did not include all of the observed targets in 2012 because of our inability to unambiguously identify every KOI. Using this new method of target confirmation

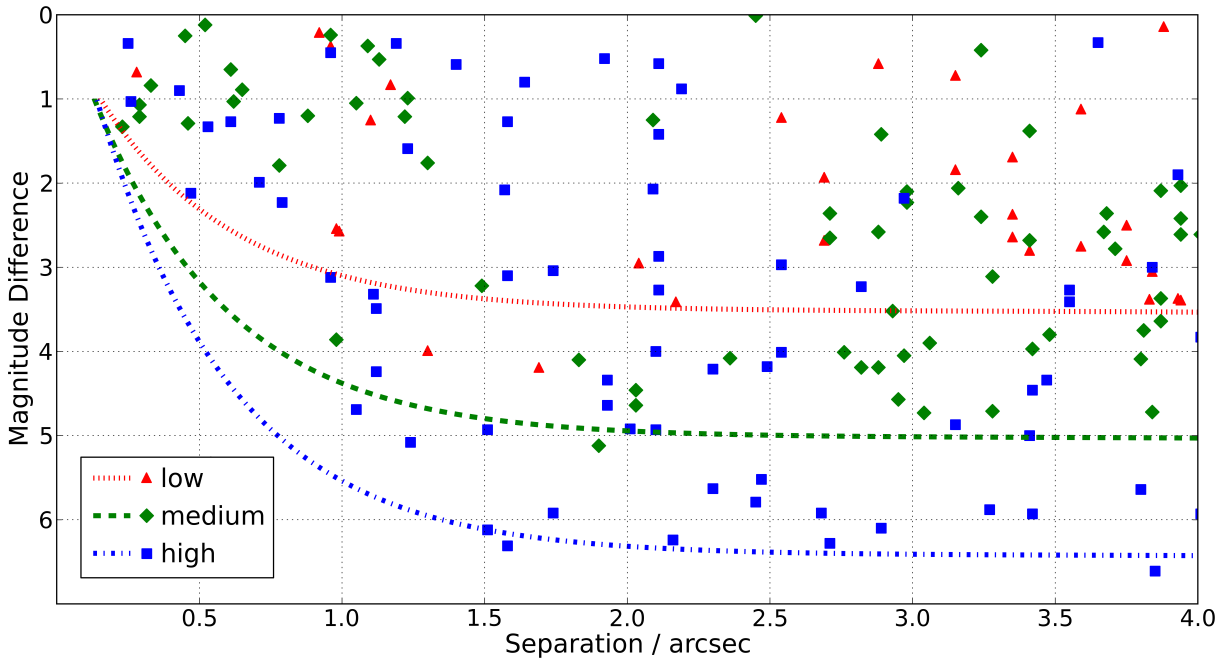

Figure 2. The points on this plot show the angular separations and magnitude differences of the detected companions described in Tables 2 and 3, with the color and shape of each point denoting the associated typical low-, medium- and high-performance 5σ contrast curve during the observation (as described in Section 3.5).

we were able to positively identify 13 KOIs observed in 2012 and now include them in this paper.

3.2. *Imaging Pipeline*

The Robo-AO imaging pipeline (Law et al. 2012; Terziev et al. 2013) is based on the lucky imaging reduction system described in Law et al. (2006a,b, 2009). The recorded camera frames are dark-subtracted and flat-fielded, and are then corrected for image displacement using the KOI as the reference guide star. This produced more consistent and predictable imaging performance for groups of similar KOIs, even if a brighter guide star was nearby and offered potentially increased performance.

3.3. *PSF Subtraction*

The large number of KOI target stars observed each night are all in similar parts of the sky, have similar brightness, and were observed at similar airmasses. We take advantage of this fact and use each night's KOI observations as PSF references due to the fact that it is unlikely that a companion would be in the same position for multiple targets. We use a custom locally optimized PSF subtraction routine based on the Locally Optimized Combination of Images algorithm (Lafrenière et al. 2007), wherein the regions around at least 20 targets are combined to create a PSF which is an optimal local combination of the reference PSFs and is then subtracted from the target star's PSF. The PSF subtraction typically leaves residuals that are consistent with photon noise only (for these relatively short exposures). For more information and an example of the target star subtraction see Paper I.

3.4. *Automated Companion Detection*

To more easily and robustly find companions in this large data set, we developed a new automated companion detection algorithm for Robo-AO data, described in Paper I. During the analysis of images for this survey we extended the automated search radius from $2\farcs5$ to $4\farcs0$ to capture a larger population of stars that contribute to the *Kepler* light curves, as well as to facilitate better comparison with other high-angular-resolution imaging surveys.

We also manually checked each image for companions after the automated companion detection to assess the performance of the automated system and to search for faint but real companions that could have been removed by spurious speckles in the PSF references. Only those that had a measured significance of $> 2.0\sigma$ are reported here despite the fact that others may have confirmed their existence (e.g., the $\sim 0\farcs5$ companions detected near KOI-3284 and KOI-3309). While not comprehensive, we also flagged several low-significance companions out to $\sim 4\farcs5$ that were just outside of the automatic search radius during the manual check.

3.5. *Imaging Performance Metrics*

In Paper I, we evaluated the contrast-versus-radius detection performance of the PSF-subtraction and automated companion detection code by performing Monte Carlo simulations of artificial companion injection and recovery. We found that if we fit two Moffat functions to each PSF, one tuned to the PSF core and the other to the uncorrected halo, that the width of the PSF core size alone was an excellent predictor of contrast performance. On this basis, we used the PSF core size to assign targets to contrast-performance groups: 'low', $<0\farcs1$, N=355; 'medium', $[0\farcs1, 0\farcs14)$, N=308; and 'high', $\geq 0\farcs14$, N=306. Figure 2 shows smoothed contrast curves resulting from the Monte Carlo companion-detection simulations for the three ranges of contrast-

performance groups.

3.6. *Companion Contrast Ratios, Separations and Position Angles*

We determined the contrast ratio between the companions and primaries in two ways: for the widest separations we performed aperture photometry on the original images; for the closer systems we used the estimated PSF to remove the blended contributions of each of the stars before performing aperture photometry. In all cases the aperture sizes were optimized for the system separation and the available signal. We calculated the contrast ratio uncertainty on the basis of the difference between the injected and measured contrasts of the artificial companions during the contrast-curve calculations (Section 3.4). We found that the detection significance of the companion was the best predictor of the contrast ratio accuracy, and so we use that relation to estimate the contrast ratio uncertainty for each companion. We note that the uncertainties (5%-30%) are much higher than would be naively expected from the S/N of the companion detection, as they include an estimate of the systematic errors resulting from the AO imaging, PSF-subtraction and contrast-measurement processes.

To obtain the separation and position angle of the binaries we measured the centroid of the PSF-subtracted images of the companion and primary, as above. We converted the raw pixel positions to on-sky separations and position angles using a distortion solution produced from Robo-AO measurements of globular clusters, detailed in Riddle et al. (2015). We calculated the uncertainties of the companion separation and position angles using estimated systematic errors in the position measurements due to blending between components, depending on the separation of the companion (typically 1-2 pixels uncertainty in the position of each star). We also included an estimate of the maximal changes in the Robo-AO orientation throughout the observation period ($\pm1\overset{\circ}{.}5$), as verified using the globular cluster measurements above. Finally, we verified the measured positions and contrast ratios in direct measurement from non-PSF-subtracted images.

4. NIRC2 DATA REDUCTION

We created a pipeline to automatically reduce and analyze our NIRC2 data. After sky subtraction and flat-field calibration, the frames were co-added into a single image based on the automatic detection of the location of the primary star in each dither frame. Because the distortion across each detector quadrant is sufficiently small compared to the Robo-AO position errors, $\leq$20mas (Yelda et al. 2010), we did not correct for field distortion. The pipeline then automatically identifies companion stars via pixel binning, vetting the brightest bins by measuring radius in the eight cardinal and diagonal directions against a minimum cutoff and radial consistency. Cutoff values are optimized to search for both wide and narrow separation companions. For targets with observations in multiple filters (reported in D. Atkinson et al., 2016, in preparation), the results are cross-referenced and stars found in only one filter are dropped as multi-color observations are effective in discriminating PSF speckles from astrophysical objects. Targets for which the pipeline registered multiple companions are flagged for manual validation.

The higher angular resolution images clearly separate the vast majority of companions and simple aperture photometry is used to measure the brightness of each star. For close companions, a matching aperture opposite the partner star from the object being investigated is subtracted from the star's own photometry. This corrects for any overlapping PSF halo (and assumes a radially constant PSF, which is more accurate at larger separations). Magnitude differences between companions and their primary star are shown in Table 4.

The uncertainty in the magnitude difference is estimated by varying the aperture radius from 0.5 to 5 of the width of the stellar PSF and measuring the standard deviation of the difference. Injected companions are used to measure the overall efficacy of the technique and determine the weighting of magnitude difference vs. aperture radius. Recovering injections with this technique demonstrated an uncertainty of $\sim$ 5%, consistent with our reported uncertainties.

5. DISCOVERIES

We resolved 181 Kepler planet candidate hosts into multiple stars; the contrast ratios and the separations are shown in Figure 2 and the discovery images are summarized in Figures 3-5. The measured companion properties for the targets with secure detections, $> 5\sigma$, are detailed in Table 2. Table 3 describes probable companions which fell just below our formal 5σ detection criteria. We consider these very likely to be real, but we cannot exclude the possibility that a small fraction of these detections are spurious speckles without additional information. Where possible we observed these targets with NIRC2 to confirm their existence as discussed in Section 5.3.

5.1. *Comparison to Other Imaging Surveys*

In the search for blended *Kepler* companions, many other high-angular-resolution surveys of KOIs have been performed using a range of observational techniques, e.g., infrared adaptive optics, sparse aperture interferometry, speckle interferometry, lucky imaging and direct imaging with HST (Adams et al. 2012, 2013; Dressing et al. 2014; Everett et al. 2015; Gaidos et al. 2016; Gilliland et al. 2015; Howell et al. 2011; Horch et al. 2012; Kraus et al. 2016; Lillo-Box et al. 2012, 2014; Marcy et al. 2014; Teske et al. 2015; Torres et al. 2015; Wang et al. 2015a,b). Each technique and instrument setup has a unique sensitivity, inner working angle, and spectral bandpass, presenting a challenge for a complete analysis of the multiplicity of KOI stars, and is part of our motivation for observing all KOIs with a single instrument setup. We have indicated in Tables 2 and 3 where these surveys have previously detected the same companion at approximately the same location. These other surveys have detected 38 of the 98 companions we detected at a significance greater than 5σ, and 24 of the 105 companions we detected at a lower significance.

Interestingly, Robo-AO was able to detect a close companion to KOI-2971 at a significance of 3.9σ that was not detected by Dressing et al. (2014) using ARIES with the MMT AO system; and conversely Robo-AO did not detect the $3\overset{''}{.}5$ companion found by Dressing et al. (2014).

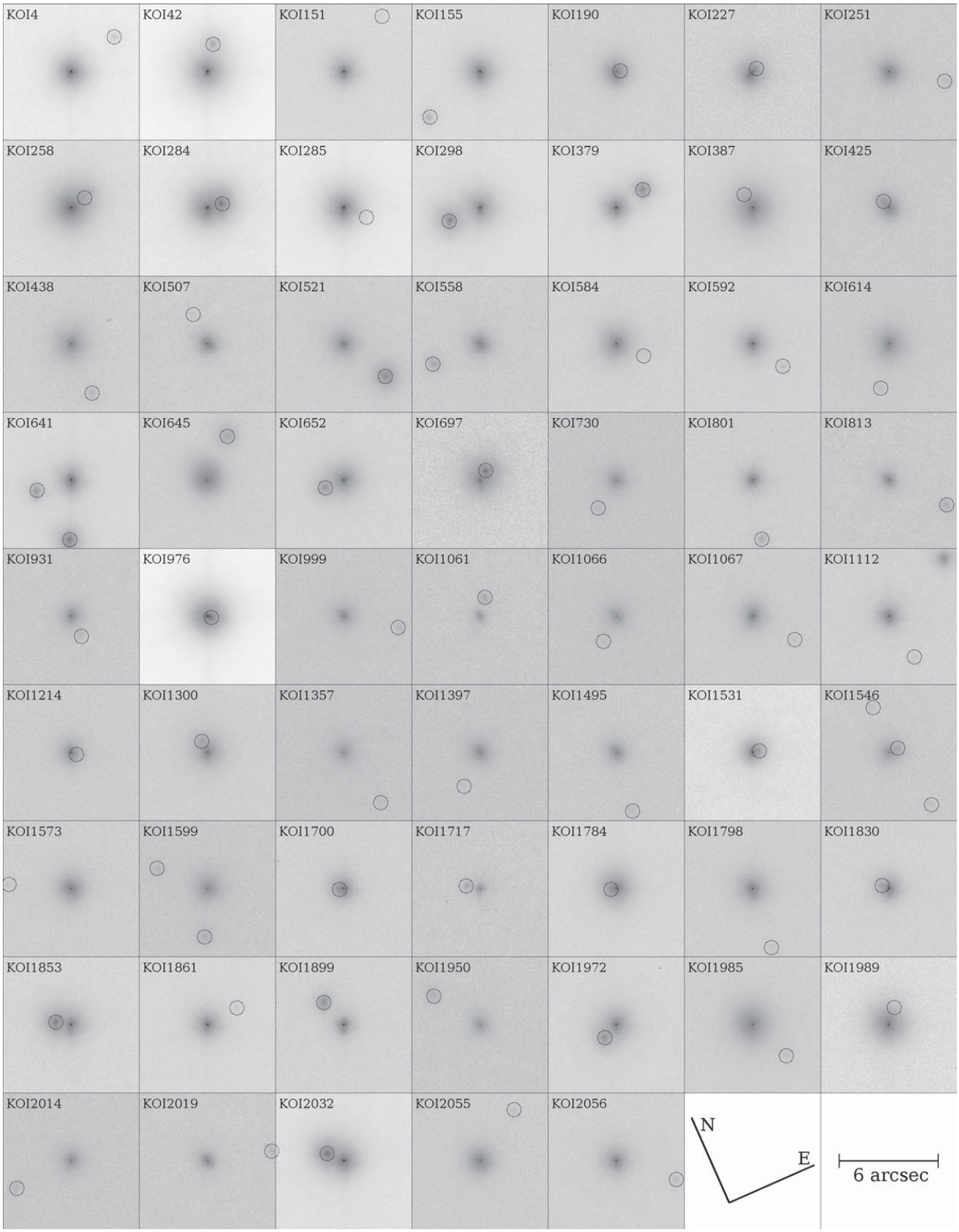

Figure 3. Color inverted, normalized log-scale cutouts of 61 multiple KOI systems [KOI-4 to KOI-2056] with separations <4″ resolved with Robo-AO. The angular scale and orientation is similar for each cutout. The smaller circles are centered on the detected nearby star.

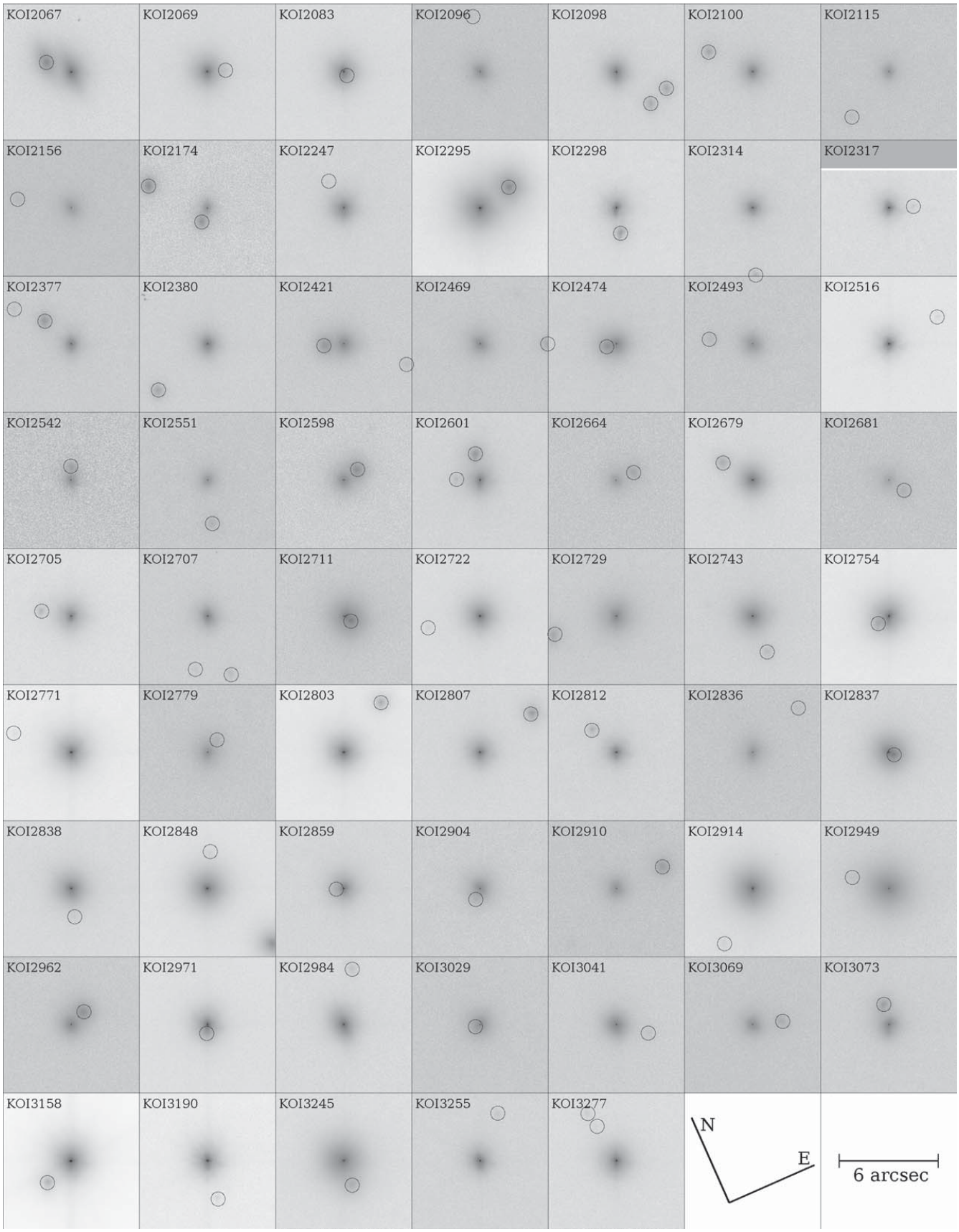

Figure 4. Color inverted, normalized log-scale cutouts of 61 multiple KOI systems [KOI-2067 to KOI-3277] with separations <4″ resolved with Robo-AO. The angular scale and orientation is similar for each cutout. The smaller circles are centered on the detected nearby star.

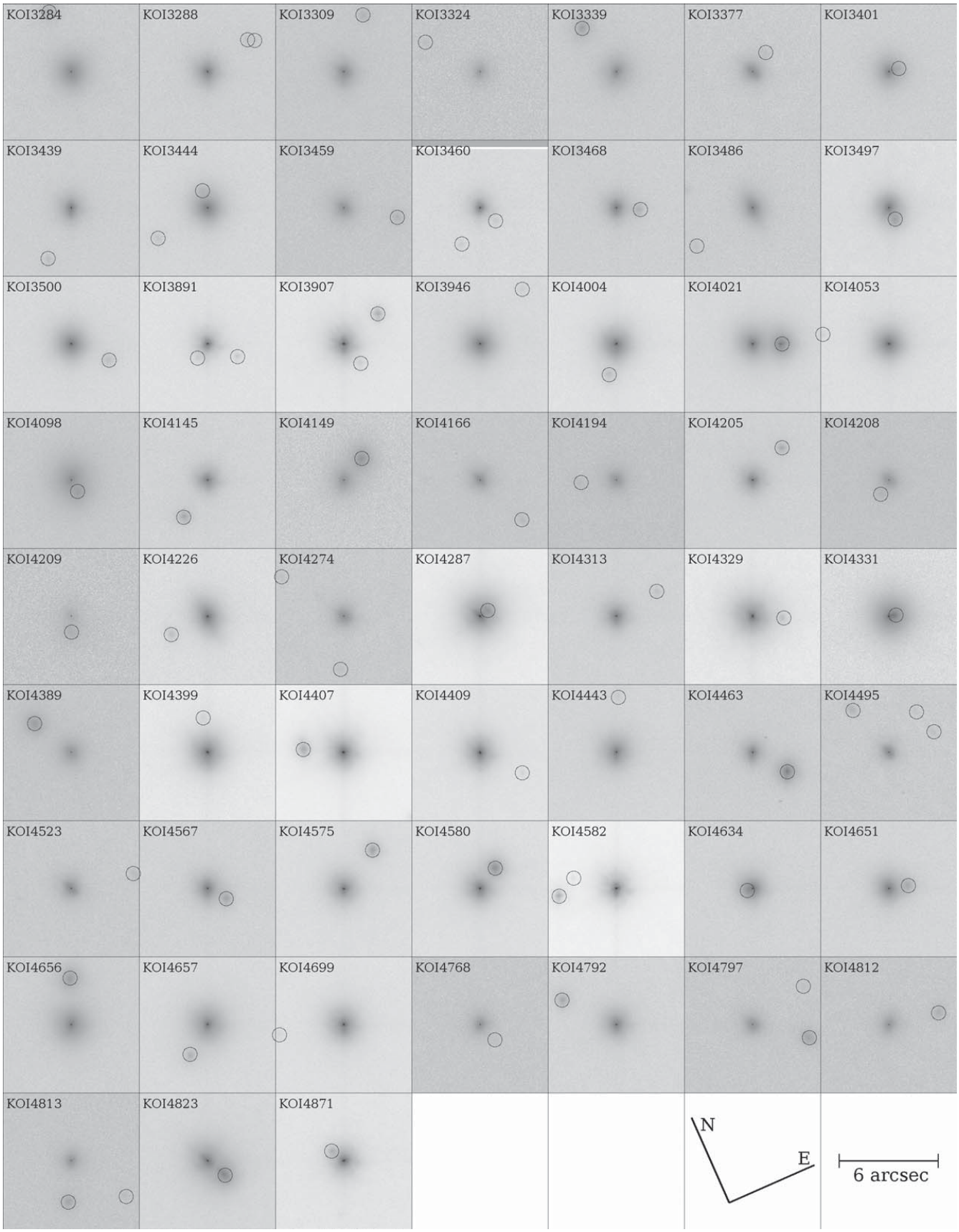

Figure 5. Color inverted, normalized log-scale cutouts of 59 multiple KOI systems [KOI-3284 to KOI-4871] with separations <4″ resolved with Robo-AO. The angular scale and orientation is similar for each cutout. The smaller circles are centered on the detected nearby star.

We fortuitously observed KOI-2971 with NIRC2 (see Section 5.3) and we were able to clearly see both of these companions.

We also note that the Robo-AO automated companion detection software found companions to KOI-2849 and KOI-3246 at nearly the same separation, 0.″36, position angle, 215°, magnitude difference, ∼ 1, and at a significance level of 4.0 σ and 5 σ respectively. Observations of both targets occurred on 2013 August 16 and showed evidence of static non-common path error in the stellar PSF leading to a speckle in the position of the purported companions. Kraus et al. (2016) observed KOI-3246 with NIRC2, and confirmed that there was no companion of similar brightness near the location of the Robo-AO automated detection. Because of our insensitivity at that position during that night we did not report these detections in our list of companions.

5.2. *Comparison to a Spectroscopic Survey*

Kolbl et al. (2015) searched for close companions to KOIs by detecting secondary light sources in spectra used for determining radial velocities. They demonstrated sensitivity to companions as faint as ∼1% of the primary star, and to companions captured within the 0.″87 × 3.″0 Keck-HIRES entrance slit. We observed 19 of the 58 KOIs for which Kolbl et al. (2015) found evidence for a companion. Of those 19, we detected companions to KOI-151, KOI-652, KOI-1784 and KOI-4871. We had sufficient image contrast performance for the other 15 targets, 12 'high' and 3 'medium', to detect the brightness of companion indicated by Kolbl et al. (2015) if they were separated by greater than roughly 0.″75; this lends evidence to the spectroscopic companions existing at closer angular separations.

We detected a companion to KOI-151 at an angular separation of 4.″2 and at a radiant flux ratio of 0.0046±0.0008 with respect to the primary star. This companion is fainter than the 1σ lower limit on the radiant flux of 0.012±0.006 determined by Kolbl et al. (2015) and was likely not captured by the HIRES entrance slit. Therefore we conclude that our detection is new and that KOI-151 is an asterism of at least three stars.

We detected a companion to KOI-652 at an angular separation of 1.″23. This companion was also detected by Teske et al. (2015) and Kraus et al. (2016) with Keck-NIRC2 as a ∼0.″08 binary. This lends further evidence to Kolbl et al.'s claim that this system is at least a triple star system.

Both we and Wang et al. (2015b) detected a companion to KOI-1784 at an angular separation of ∼0.″3, which would easily be captured within the HIRES entrance slit. We calculate a radiant flux ratio of 0.59±0.07 which is well above the lower limit of 0.192±0.058 determined by Kolbl et al. (2015). Wang et al. (2015b) estimated a physical separation of 160.7 AU between the primary and the companion, and this may not be compatible with the ΔRV of -13 km s^{-1} measured by Kolbl et al. (2015). It is not conclusive that the imaged close companion is also responsible for the spectroscopic signal, so it is possible this is also an asterism of at least three stars.

We observed a companion to KOI-4871 at an angular separation of 0.″96 and a radiant flux ratio of 0.057±0.010 with respect to the primary star. This detection is compatible with the lower limit on the radiant flux ratio of 0.012±0.003 determined by Kolbl et al. (2015). If this is indeed the same star, Kolbl et al.'s reported ΔRV of -23 km s^{-1} suggests it is not physically associated with the primary.

While we have not conclusively imaged stellar companions that were detected by Kolbl et al.'s survey, we have found additional nearby stars not detected by spectroscopic methods. As previously suggested by Teske et al. (2015), spectroscopic and AO methods can probe complementary, and sometimes overlapping, regions of parameter space when searching for stellar companions. While spectroscopic companions can be detected at much closer angular separations, AO observations probe larger angular separations, and at a much greater dynamic range that can be used to more precisely calibrate transit radii measurements. Physical association of companions can be established either from the difference in measured radial velocities from spectroscopy or from probabilistic or additional spectrophotometric parallax analysis when using AO. From a practical perspective, adaptive optics imaging requires much less on-sky observing time, and can target a much greater range of exoplanetary host stars.

5.3. *Keck-NIRC2 imaging of Robo-AO observed KOIs*

Details of the 50 observations and 63 companions detected with NIRC2 appear in Table 4. We observed 14 KOIs with companions detected at $> 5\sigma$ so we could later calculate spectrophotometric parallax distances to determine the probability of physical association. We observed 13 companions detected by Paper I at a significance level of $< 5\sigma$. Including those previously imaged with NIRC2 and by Lillo-Box et al. (2012); Adams et al. (2012), all 17 of these detections have been confirmed.

The remainder of KOIs we observed with NIRC2 were at various levels of analysis: some Robo-AO images had been fully processed with measured significance levels on the candidate companion, others were manually identified before PSF subtraction. We confirmed 24 of the companions detected at a significance level of $< 5\sigma$ in this survey (2 of which were in systems with a $> 5\sigma$ detected companion), and other surveys confirmed 18 more of these companions. Due to the enhanced contrast with NIRC2, we found additional companions to 6 KOIs (1884, 2377, 2971, 3029, 3377 and 4407) that were not detected in the original Robo-AO data. We also found individual companions near KOI-2363 and KOI-4292 in the NIRC2 data that did not correspond to the preliminary manually-identified candidate companions in the Robo-AO data and we note them in Tables 4 and 5. Despite the somewhat haphazard selection of targets, the vast majority of Robo-AO detections that have follow-up observations with NIRC2 have been shown to be real; so far, 60 of the 120 companions detected at a significance of $< 5\sigma$ with Robo-AO from Paper I and this work have been confirmed.

6. DISCUSSION

We observed 969 Kepler planetary system candidates with the Robo-AO robotic laser adaptive optics system. Presuming all confirmed and probable 203 Robo-AO detected companions within ∼4″of 181 KOIs are real, we calculate the nearby-star probability as a function of angular distance, see Figure 7. In our previous study we

found a probability of 7.4% ± 1.0% at angular separations up to 2.″5 around 715 KOIs. For direct comparison, we calculated the probability in our sample to the same separation of 2.″5 and found it to be 10.6% ± 1.1%, a difference of 2.2 σ. Additional fainter companions are discovered here, e.g., 9 companions with a magnitude difference greater than 5 within 2.″5 compared to 3 previously.

We explored the possibility of a bias change in the KOI selection process between major data releases, Q1-Q6 (Batalha et al. 2013) and Q1-Q12 (Rowe et al. 2015). Our first study comprised 715 targets solely from Q1-Q6, while this work includes targets originally identified in both catalogs, 505 that appear in Q1-Q6 (51 of which have <2.″5 companions) and 464 that only appear in Q1-Q12 (52 companions). After combining the results of both and comparing the nearby-star probability within 2.″5 for the KOIs that only appear in Q1-Q12 catalog versus those originally found in the Q1-Q6 catalog, we find probabilities of 11.2%±1.6% and 8.5%±0.9% respectively, a difference of 1.5 σ.

We also examined the on-sky spatial distribution of observed KOIs and those with <2.″5 companions for both studies (Figure 6). In our cumulative survey there is a bias of targets located closer to the galactic plane compared to the center of the *Kepler* field. Additionally, compared to our first study, the median position of KOIs observed in this work is closer to the galactic plane by 1.1°, and the median position of KOIs with <2.″5 companions is closer to the galactic plane by 1.4°. We find in general that higher-galactic-latitude KOIs have fewer wide companions which is consistent with lower stellar crowding away from the galactic plane in the *Kepler* field (Gilliland et al. 2011), and therefore the difference in nearby star probability between this work and Paper I may simply be due to the specific KOI samples.

Previous studies have shown that the majority of stellar companions to KOIs at a separation of <1″are physically associated, with the probability of association decreasing with increasing angular separation (Horch et al. 2014). We calculate the cumulative nearby-star probability as a function of angular separation of our data and present it in Figure 7. Our data show that the probability increases nearly linearly with increasing separation, up to 17.9%±1.4% out to a separation of 4.″0. If the distribution had consisted solely of chance alignments of non-physically associated companions, we would expect this probability to instead increase quadratically. This suggests again that a large fraction of the companions with smaller angular separations are indeed physically associated with the primary star.

This work and Paper I together comprise a survey of roughly half of the KOIs in the Q1-Q17 DR24 dataset release. In light of the apparent discrepancy in companion discovery rates between the two using the same instrument, we caution against extrapolating companion rates from any individual survey that samples a small fraction of the overall population. Even when combined, the existing patchwork of other KOIs surveys (see Section 5.1) is not as comprehensive, and requires detailed calibration to match the varying sensitivities, inner working angles and wavelength ranges. Future high-angular-resolution follow-up observations of large numbers of candidate exoplanet hosts would benefit from an initial comprehensive survey from Robo-AO that can very efficiently find lower contrast blended stars; preserving precious and limited resources like Keck AO or HST for those targets that pass the initial round of vetting.

We expect that our data will be used by other researchers using *Kepler* data to study and validate exoplanets, their host stars and stellar environments, and other astrophysical phenomena. To aid in this effort, Robo-AO images of KOIs and the position and photometry of any detected companions will be available at the *Kepler* Community Follow-up Observing Program[8].

7. FUTURE WORK

In the third installment of this paper series we will present the remaining Robo-AO observations of KOIs and explore an analysis of the complete data set. We will detail the effects of the detected nearby stars on the interpretation of *Kepler* planetary candidates and note particular systems of interest. We will investigate further the spatial distribution of all KOIs with companions as a function of separation.

In parallel, we are currently using the multi-color visible and infrared observations obtained for this survey to estimate relative spectrophotometric distances between KOIs and their detected companions to determine if the stars are physically bound. We have also inspected all of our Robo-AO images of KOIs for images of other *Kepler* input catalog (KIC) targets that do not have repeating transit signals. We have identified nearly 700 of these serendipitously observed KICs in our existing data; we will use these observations as a control sample to determine if there is a fundamental difference in the nearby-star probability between the KOIs and non-KOI KICs, including if there are similar effects due to galactic latitude, and whether this has an effect on planetary systems (Nofi et al. 2015).

We have reconfigured and redeployed the Robo-AO system as the only instrument on the 2.1-m telescope at Kitt Peak as of November 2015 (Riddle et al. 2016). We intend to continue observations of our detected companions to search for common-proper-motion pairs to better understand the probability of physical association. We will additionally integrate a science-grade-detector version of a low-noise infrared camera to Robo-AO (previously demonstrated by Baranec et al. 2015). This camera will enable both infrared imaging and tip-tilt sensing and correction that will allow us to better observe redder KOIs.

We are also in the process of building an upgraded Robo-AO system for the University of Hawai'i 2.2-m telescope on Maunakea (Baranec et al. 2014a). Between the two Robo-AO systems, we will be able observe up to ∼500 objects per night, covering nearly three-quarters of the sky over the course of a year. Forthcoming transit missions such as NASA's Transiting Exoplanet Survey Satellite (Ricker et al. 2015) scheduled to launch in 2017, and ESA's PLAnetary Transits and Oscillations of stars 2.0 (Rauer et al. 2014) will release their data on timescales of months and shorter, and are expected to discover a greater number of exoplanet systems compared to *Kepler*. Only the extremely efficient and rapid follow-up capability of Robo-AO will be able to keep up

[8] See https://exofop.ipac.caltech.edu/cfop.php

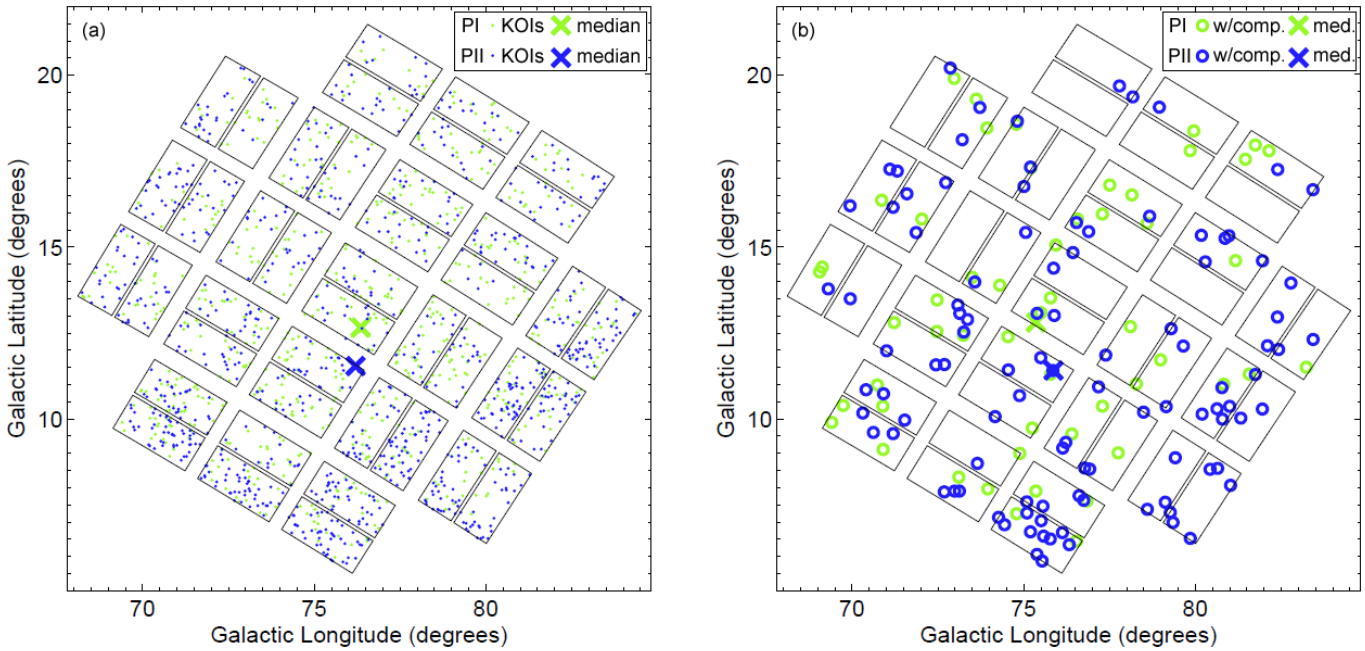

Figure 6. Location in galactic coordinates for the KOIs (a), and those with companions detected at angular separations of less than 2.″5 (b), observed by Paper I (PI) and in this work (PII). In both figures the '×' represents the median galactic coordinate for each set of objects. Projections of the *Kepler* detectors on sky for the Spring season is provided for reference.

with the sustained demand for high-acuity imaging of thousands of exoplanet candidate host stars identified by these and other projects.

This research is supported by the NASA Exoplanets Research Program, grant #NNX 15AC91G. C.B. acknowledges support from the Alfred P. Sloan Foundation. T.M. is supported by NASA grant #NNX 14AE11G under the Kepler Participating Scientist Program. D.A. is supported by a NASA Space Technology Research Fellowship, grant #NNX 13AL75H.

The Robo-AO system was developed by collaborating partner institutions, the California Institute of Technology and the Inter-University Centre for Astronomy and Astrophysics, and with the support of the National Science Foundation under Grant Nos. AST-0906060, AST-0960343, and AST-1207891, the Mt. Cuba Astronomical Foundation and by a gift from Samuel Oschin. We are grateful to the Palomar Observatory staff for their support of Robo-AO on the 1.5 m telescope, particularly S. Kunsman, M. Doyle, J. Henning, R. Walters, G. Van Idsinga, B. Baker, K. Dunscombe and D. Roderick. We thank Adam Kraus et al. for sharing a preprint of their paper. This work used the astronomy & astrophysics package for Matlab (Ofek 2014). Some of the data presented herein were obtained at the W.M. Keck Observatory, which is operated as a scientific partnership among the California Institute of Technology, the University of California and the National Aeronautics and Space Administration. The Observatory was made possible by the generous financial support of the W.M. Keck Foundation. The authors wish to recognize and acknowledge the very significant cultural role and reverence that the summit of Maunakea has always had within the indigenous Hawaiian community. We are most fortunate to have the opportunity to conduct observations from this mountain.

Facilities: PO:1.5m (Robo-AO), Keck:II (NIRC2-LGS).

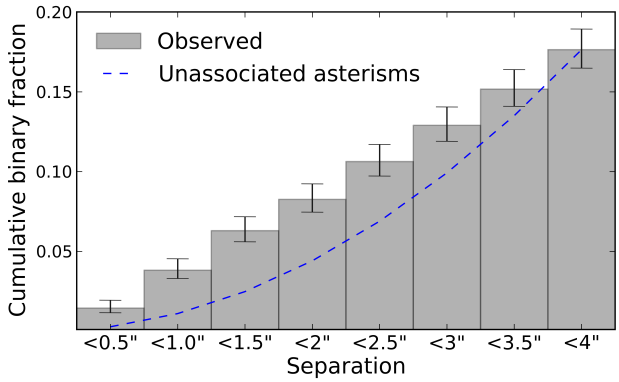

Figure 7. Cumulative companion fraction for Robo-AO observed KOIs as a function of angular separation. The dashed line represents a theoretical quadratic cumulative distribution that would be expected from non-physically associated companions.

APPENDIX

In Table 5, we list our Robo-AO observed KOIs, including date the target was observed, the observation quality as described in Section 3.5, and the presence of detected companions.

REFERENCES

Adams, E. R., Ciardi, D. R., Dupree, A. K., Gautier, III, T. N., Kulesa, C., & McCarthy, D. 2012, AJ, 144, 42
Adams, E. R., Dupree, A. K., Kulesa, C., & McCarthy, D. 2013, AJ, 146, 9

Akeson, R. L., Chen, X., Ciardi, D., Crane, M., Good, J., Harbut, M., Jackson, E., Kane, S. R., Laity, A. C., Leifer, S., Lynn, M., McElroy, D. L., Papin, M., Plavchan, P., Ramírez, S. V., Rey, R., von Braun, K., Wittman, M., Abajian, M., Ali, B., Beichman, C., Beekley, A., Berriman, G. B., Berukoff, S., Bryden, G., Chan, B., Groom, S., Lau, C., Payne, A. N., Regelson, M., Saucedo, M., Schmitz, M., Stauffer, J., Wyatt, P., & Zhang, A. 2013, PASP, 125, 989

Baranec, C., Atkinson, D., Riddle, R., Hall, D., Jacobson, S., Law, N. M., & Chun, M. 2015, ApJ, 809, 70

Baranec, C., Riddle, R., Law, N. M., Chun, M. R., Lu, J. R., Connelley, M. S., Hall, D., Atkinson, D., & Jacobson, S. 2014a, in Proc. SPIE, Vol. 9148, Adaptive Optics Systems IV, 914812

Baranec, C., Riddle, R., Law, N. M., Ramaprakash, A. N., Tendulkar, S. P., Bui, K., Burse, M. P., Chordia, P., Das, H. K., Davis, J. T. C., Dekany, R. G., Kasliwal, M. M., Kulkarni, S. R., Morton, T. D., Ofek, E. O., & Punnadi, S. 2013, Journal of Visualized Experiments, 72, e50021

Baranec, C., Riddle, R., Law, N. M., Ramaprakash, A. N., Tendulkar, S. P., Hogstrom, K., Bui, K., Burse, M., Chordia, P., Das, H., Dekany, R. G., Kulkarni, S., & Punnadi, S. 2014b, ApJ, 790, L8

Batalha, N. M., Rowe, J. F., Bryson, S. T., Barclay, T., Burke, C. J., Caldwell, D. A., Christiansen, J. L., Mullally, F., Thompson, S. E., Brown, T. M., Dupree, A. K., Fabrycky, D. C., Ford, E. B., Fortney, J. J., Gilliland, R. L., Isaacson, H., Latham, D. W., Marcy, G. W., Quinn, S. N., Ragozzine, D., Shporer, A., Borucki, W. J., Ciardi, D. R., Gautier, III, T. N., Haas, M. R., Jenkins, J. M., Koch, D. G., Lissauer, J. J., Rapin, W., Basri, G. S., Boss, A. P., Buchhave, L. A., Carter, J. A., Charbonneau, D., Christensen-Dalsgaard, J., Clarke, B. D., Cochran, W. D., Demory, B.-O., Desert, J.-M., Devore, E., Doyle, L. R., Esquerdo, G. A., Everett, M., Fressin, F., Geary, J. C., Girouard, F. R., Gould, A., Hall, J. R., Holman, M. J., Howard, A. W., Howell, S. B., Ibrahim, K. A., Kinemuchi, K., Kjeldsen, H., Klaus, T. C., Li, J., Lucas, P. W., Meibom, S., Morris, R. L., Prša, A., Quintana, E., Sanderfer, D. T., Sasselov, D., Seader, S. E., Smith, J. C., Steffen, J. H., Still, M., Stumpe, M. C., Tarter, J. C., Tenenbaum, P., Torres, G., Twicken, J. D., Uddin, K., Van Cleve, J., Walkowicz, L., & Welsh, W. F. 2013, ApJS, 204, 24

Campante, T. L., Barclay, T., Swift, J. J., Huber, D., Adibekyan, V. Z., Cochran, W., Burke, C. J., Isaacson, H., Quintana, E. V., Davies, G. R., Silva Aguirre, V., Ragozzine, D., Riddle, R., Baranec, C., Basu, S., Chaplin, W. J., Christensen-Dalsgaard, J., Metcalfe, T. S., Bedding, T. R., Handberg, R., Stello, D., Brewer, J. M., Hekker, S., Karoff, C., Kolbl, R., Law, N. M., Lundkvist, M., Miglio, A., Rowe, J. F., Santos, N. C., Van Laerhoven, C., Arentoft, T., Elsworth, Y. P., Fischer, D. A., Kawaler, S. D., Kjeldsen, H., Lund, M. N., Marcy, G. W., Sousa, S. G., Sozzetti, A., & White, T. R. 2015, ApJ, 799, 170

Cenko, S. B., Fox, D. B., Moon, D.-S., Harrison, F. A., Kulkarni, S. R., Henning, J. R., Guzman, C. D., Bonati, M., Smith, R. M., Thicksten, R. P., Doyle, M. W., Petrie, H. L., Gal-Yam, A., Soderberg, A. M., Anagnostou, N. L., & Laity, A. C. 2006, The Publications of the Astronomical Society of the Pacific, 118, 1396

Ciardi, D. R., Beichman, C. A., Horch, E. P., & Howell, S. B. 2015, ApJ, 805, 16

Coughlin, J. L., Mullally, F., Thompson, S. E., Rowe, J. F., Burke, C. J., Latham, D. W., Batalha, N. M., Ofir, A., Quarles, B. L., Henze, C. E., Wolfgang, A., Caldwell, D. A., Bryson, S. T., Shporer, A., Catanzarite, J., Akeson, R., Barclay, T., Borucki, W. J., Boyajian, T. S., Campbell, J. R., Christiansen, J. L., Girouard, F. R., Haas, M. R., Howell, S. B., Huber, D., Jenkins, J. M., Li, J., Patil-Sabale, A., Quintana, E. V., Ramirez, S., Seader, S., Smith, J. C., Tenenbaum, P., Twicken, J. D., & Zamudio, K. A. 2015, ArXiv e-prints

Dressing, C. D., Adams, E. R., Dupree, A. K., Kulesa, C., & McCarthy, D. 2014, AJ, 148, 78

Dressing, C. D. & Charbonneau, D. 2013, ApJ, 767, 95

Everett, M. E., Barclay, T., Ciardi, D. R., Horch, E. P., Howell, S. B., Crepp, J. R., & Silva, D. R. 2015, AJ, 149, 55

Fressin, F., Torres, G., Charbonneau, D., Bryson, S. T., Christiansen, J., Dressing, C. D., Jenkins, J. M., Walkowicz, L. M., & Batalha, N. M. 2013, ApJ, 766, 81

Gaidos, E., Mann, A. W., Kraus, A. L., & Ireland, M. 2016, MNRAS, in press

Gilliland, R. L., Cartier, K. M. S., Adams, E. R., Ciardi, D. R., Kalas, P., & Wright, J. T. 2015, AJ, 149, 24

Gilliland, R. L., Chaplin, W. J., Dunham, E. W., Argabright, V. S., Borucki, W. J., Basri, G., Bryson, S. T., Buzasi, D. L., Caldwell, D. A., Elsworth, Y. P., Jenkins, J. M., Koch, D. G., Kolodziejczak, J., Miglio, A., van Cleve, J., Walkowicz, L. M., & Welsh, W. F. 2011, ApJS, 197, 6

Haas, M. R., Batalha, N. M., Bryson, S. T., Caldwell, D. A., Dotson, J. L., Hall, J., Jenkins, J. M., Klaus, T. C., Koch, D. G., Kolodziejczak, J., Middour, C., Smith, M., Sobeck, C. K., Stober, J., Thompson, R. S., & Van Cleve, J. E. 2010, ApJ, 713, L115

Horch, E. P., Howell, S. B., Everett, M. E., & Ciardi, D. R. 2012, AJ, 144, 165

—. 2014, ApJ, 795, 60

Howell, S. B., Everett, M. E., Sherry, W., Horch, E., & Ciardi, D. R. 2011, AJ, 142, 19

Kolbl, R., Marcy, G. W., Isaacson, H., & Howard, A. W. 2015, AJ, 149, 18

Kraus, A. L., Ireland, M. J., Huber, D., Mann, A. W., & Dupuy, T. J. 2016, ApJ, in press

Lafrenière, D., Marois, C., Doyon, R., Nadeau, D., & Artigau, É. 2007, ApJ, 660, 770

Law, N. M., Hodgkin, S. T., & Mackay, C. D. 2006a, MNRAS, 368, 1917

Law, N. M., Kraus, A. L., Street, R., Fulton, B. J., Hillenbrand, L. A., Shporer, A., Lister, T., Baranec, C., Bloom, J. S., Bui, K., Burse, M. P., Cenko, S. B., Das, H. K., Davis, J. T. C., Dekany, R. G., Filippenko, A. V., Kasliwal, M. M., Kulkarni, S. R., Nugent, P., Ofek, E. O., Poznanski, D., Quimby, R. M., Ramaprakash, A. N., Riddle, R., Silverman, J. M., Sivanandam, S., & Tendulkar, S. P. 2012, ApJ, 757, 133

Law, N. M., Mackay, C. D., & Baldwin, J. E. 2006b, A&A, 446, 739

Law, N. M., Mackay, C. D., Dekany, R. G., Ireland, M., Lloyd, J. P., Moore, A. M., Robertson, J. G., Tuthill, P., & Woodruff, H. C. 2009, ApJ, 692, 924

Law, N. M., Morton, T., Baranec, C., Riddle, R., Ravichandran, G., Ziegler, C., Johnson, J. A., Tendulkar, S. P., Bui, K., Burse, M. P., Das, H. K., Dekany, R. G., Kulkarni, S., Punnadi, S., & Ramaprakash, A. N. 2014, ApJ, 791, 35

Lillo-Box, J., Barrado, D., & Bouy, H. 2012, A&A, 546, A10

—. 2014, A&A, 566, A103

Marcy, G. W., Isaacson, H., Howard, A. W., Rowe, J. F., Jenkins, J. M., Bryson, S. T., Latham, D. W., Howell, S. B., Gautier, III, T. N., Batalha, N. M., Rogers, L., Ciardi, D., Fischer, D. A., Gilliland, R. L., Kjeldsen, H., Christensen-Dalsgaard, J., Huber, D., Chaplin, W. J., Basu, S., Buchhave, L. A., Quinn, S. N., Borucki, W. J., Koch, D. G., Hunter, R., Caldwell, D. A., Van Cleve, J., Kolbl, R., Weiss, L. M., Petigura, E., Seager, S., Morton, T., Johnson, J. A., Ballard, S., Burke, C., Cochran, W. D., Endl, M., MacQueen, P., Everett, M. E., Lissauer, J. J., Ford, E. B., Torres, G., Fressin, F., Brown, T. M., Steffen, J. H., Charbonneau, D., Basri, G. S., Sasselov, D. D., Winn, J., Sanchis-Ojeda, R., Christiansen, J., Adams, E., Henze, C., Dupree, A., Fabrycky, D. C., Fortney, J. J., Tarter, J., Holman, M. J., Tenenbaum, P., Shporer, A., Lucas, P. W., Welsh, W. F., Orosz, J. A., Bedding, T. R., Campante, T. L., Davies, G. R., Elsworth, Y., Handberg, R., Hekker, S., Karoff, C., Kawaler, S. D., Lund, M. N., Lundkvist, M., Metcalfe, T. S., Miglio, A., Silva Aguirre, V., Stello, D., White, T. R., Boss, A., Devore, E., Gould, A., Prsa, A., Agol, E., Barclay, T., Coughlin, J., Brugamyer, E., Mullally, F., Quintana, E. V., Still, M., Thompson, S. E., Morrison, D., Twicken, J. D., Désert, J.-M., Carter, J., Crepp, J. R., Hébrard, G., Santerne, A., Moutou, C., Sobeck, C., Hudgins, D., Haas, M. R., Robertson, P., Lillo-Box, J., & Barrado, D. 2014, ApJS, 210, 20

Montet, B. T., Johnson, J. A., Muirhead, P. S., Villar, A., Vassallo, C., Baranec, C., Law, N. M., Riddle, R., Marcy, G. W., Howard, A. W., & Isaacson, H. 2015, ApJ, 800, 134

Morton, T. D. & Johnson, J. A. 2011, ApJ, 738, 170

Muirhead, P. S., Becker, J., Feiden, G. A., Rojas-Ayala, B., Vanderburg, A., Price, E. M., Thorp, R., Law, N. M., Riddle, R., Baranec, C., Hamren, K., Schlawin, E., Covey, K. R., Johnson, J. A., & Lloyd, J. P. 2014, ApJS, 213, 5

Muirhead, P. S., Vanderburg, A., Shporer, A., Becker, J., Swift, J. J., Lloyd, J. P., Fuller, J., Zhao, M., Hinkley, S., Pineda, J. S., Bottom, M., Howard, A. W., von Braun, K., Boyajian, T. S., Law, N., Baranec, C., Riddle, R., Ramaprakash, A. N., Tendulkar, S. P., Bui, K., Burse, M., Chordia, P., Das, H., Dekany, R., Punnadi, S., & Johnson, J. A. 2013, ApJ, 767, 111

Nofi, L., Baranec, C., Howard, A., Riddle, R., Law, N., & Ziegler, C. 2015, in AAS/Division for Extreme Solar Systems Abstracts, Vol. 3, AAS/Division for Extreme Solar Systems Abstracts, 117.13

Ofek, E. O. 2014, MATLAB package for astronomy and astrophysics, Astrophysics Source Code Library

Rauer, H., Catala, C., Aerts, C., Appourchaux, T., Benz, W., Brandeker, A., Christensen-Dalsgaard, J., Deleuil, M., Gizon, L., Goupil, M.-J., Güdel, M., Janot-Pacheco, E., Mas-Hesse, M., Pagano, I., Piotto, G., Pollacco, D., Santos, Ċ., Smith, A., Suárez, J.-C., Szabó, R., Udry, S., Adibekyan, V., Alibert, Y., Almenara, J.-M., Amaro-Seoane, P., Eiff, M. A.-v., Asplund, M., Antonello, E., Barnes, S., Baudin, F., Belkacem, K., Bergemann, M., Bihain, G., Birch, A. C., Bonfils, X., Boisse, I., Bonomo, A. S., Borsa, F., Brandão, I. M., Brocato, E., Brun, S., Burleigh, M., Burston, R., Cabrera, J., Cassisi, S., Chaplin, W., Charpinet, S., Chiappini, C., Church, R. P., Csizmadia, S., Cunha, M., Damasso, M., Davies, M. B., Deeg, H. J., Díaz, R. F., Dreizler, S., Dreyer, C., Eggenberger, P., Ehrenreich, D., Eigmüller, P., Erikson, A., Farmer, R., Feltzing, S., de Oliveira Fialho, F., Figueira, P., Forveille, T., Fridlund, M., García, R. A., Giommi, P., Giuffrida, G., Godolt, M., Gomes da Silva, J., Granzer, T., Grenfell, J. L., Grotsch-Noels, A., Günther, E., Haswell, C. A., Hatzes, A. P., Hébrard, G., Hekker, S., Helled, R., Heng, K., Jenkins, J. M., Johansen, A., Khodachenko, M. L., Kislyakova, K. G., Kley, W., Kolb, U., Krivova, N., Kupka, F., Lammer, H., Lanza, A. F., Lebreton, Y., Magrin, D., Marcos-Arenal, P., Marrese, P. M., Marques, J. P., Martins, J., Mathis, S., Mathur, S., Messina, S., Miglio, A., Montalban, J., Montalto, M., Monteiro, M. J. P. F. G., Moradi, H., Moravveji, E., Mordasini, C., Morel, T., Mortier, A., Nascimbeni, V., Nelson, R. P., Nielsen, M. B., Noack, L., Norton, A. J., Ofir, A., Oshagh, M., Ouazzani, R.-M., Pápics, P., Parro, V. C., Petit, P., Plez, B., Poretti, E., Quirrenbach, A., Ragazzoni, R., Raimondo, G., Rainer, M., Reese, D. R., Redmer, R., Reffert, S., Rojas-Ayala, B., Roxburgh, I. W., Salmon, S., Santerne, A., Schneider, J., Schou, J., Schuh, S., Schunker, H., Silva-Valio, A., Silvotti, R., Skillen, I., Snellen, I., Sohl, F., Sousa, S. G., Sozzetti, A., Stello, D., Strassmeier, K. G., Švanda, M., Szabó, G. M., Tkachenko, A., Valencia, D., Van Grootel, V., Vauclair, S. D., Ventura, P., Wagner, F. W., Walton, N. A., Weingrill, J., Werner, S. C., Wheatley, P. J., & Zwintz, K. 2014, Experimental Astronomy, 38, 249

Ricker, G. R., Winn, J. N., Vanderspek, R., Latham, D. W., Bakos, G. Á., Bean, J. L., Berta-Thompson, Z. K., Brown, T. M., Buchhave, L., Butler, N. R., Butler, R. P., Chaplin, W. J., Charbonneau, D., Christensen-Dalsgaard, J., Clampin, M., Deming, D., Doty, J., De Lee, N., Dressing, C., Dunham, E. W., Endl, M., Fressin, F., Ge, J., Henning, T., Holman, M. J., Howard, A. W., Ida, S., Jenkins, J. M., Jernigan, G., Johnson, J. A., Kaltenegger, L., Kawai, N., Kjeldsen, H., Laughlin, G., Levine, A. M., Lin, D., Lissauer, J. J., MacQueen, P., Marcy, G., McCullough, P. R., Morton, T. D., Narita, N., Paegert, M., Palle, E., Pepe, F., Pepper, J., Quirrenbach, A., Rinehart, S. A., Sasselov, D., Sato, B., Seager, S., Sozzetti, A., Stassun, K. G., Sullivan, P., Szentgyorgyi, A., Torres, G., Udry, S., & Villasenor, J. 2015, Journal of Astronomical Telescopes, Instruments, and Systems, 1, 014003

Riddle, R. L., Baranec, C., Law, N. M., Kulkarni, S. R., Duev, D., Ziegler, C., Jensen-Clem, R. M., Atkinson, D. E., Tanner, A. M., Zhang, C., & Ray, A. 2016, in American Astronomical Society Meeting Abstracts, Vol. 227, American Astronomical Society Meeting Abstracts, 427.03

Riddle, R. L., Hogstrom, K., Papadopoulos, A., Baranec, C., & Law, N. M. 2014, in Society of Photo-Optical Instrumentation Engineers (SPIE) Conference Series, Vol. 9152, Software and Cyberinfrastructure for Astronomy III, 91521E

Riddle, R. L., Tokovinin, A., Mason, B. D., Hartkopf, W. I., Roberts, Jr., L. C., Baranec, C., Law, N. M., Bui, K., Burse, M. P., Das, H. K., Dekany, R. G., Kulkarni, S., Punnadi, S., Ramaprakash, A. N., & Tendulkar, S. P. 2015, ApJ, 799, 4

Rowe, J. F., Coughlin, J. L., Antoci, V., Barclay, T., Batalha, N. M., Borucki, W. J., Burke, C. J., Bryson, S. T., Caldwell, D. A., Campbell, J. R., Catanzarite, J. H., Christiansen, J. L., Cochran, W., Gilliland, R. L., Girouard, F. R., Haas, M. R., Hełminiak, K. G., Henze, C. E., Hoffman, K. L., Howell, S. B., Huber, D., Hunter, R. C., Jang-Condell, H., Jenkins, J. M., Klaus, T. C., Latham, D. W., Li, J., Lissauer, J. J., McCauliff, S. D., Morris, R. L., Mullally, F., Ofir, A., Quarles, B., Quintana, E., Sabale, A., Seader, S., Shporer, A., Smith, J. C., Steffen, J. H., Still, M., Tenenbaum, P., Thompson, S. E., Twicken, J. D., Van Laerhoven, C., Wolfgang, A., & Zamudio, K. A. 2015, ApJS, 217, 16

Santerne, A., Fressin, F., Díaz, R. F., Figueira, P., Almenara, J.-M., & Santos, N. C. 2013, A&A, 557, A139

Terziev, E., Law, N. M., Arcavi, I., Baranec, C., Bloom, J. S., Bui, K., Burse, M. P., Chorida, P., Das, H. K., Dekany, R. G., Kraus, A. L., Kulkarni, S. R., Nugent, P., Ofek, E. O., Punnadi, S., Ramaprakash, A. N., Riddle, R., Sullivan, M., & Tendulkar, S. P. 2013, ApJS, 206, 18

Teske, J. K., Everett, M. E., Hirsch, L., Furlan, E., Horch, E. P., Howell, S. B., Ciardi, D. R., Gonzales, E., & Crepp, J. R. 2015, AJ, 150, 144

Torres, G., Kipping, D. M., Fressin, F., Caldwell, D. A., Twicken, J. D., Ballard, S., Batalha, N. M., Bryson, S. T., Ciardi, D. R., Henze, C. E., Howell, S. B., Isaacson, H. T., Jenkins, J. M., Muirhead, P. S., Newton, E. R., Petigura, E. A., Barclay, T., Borucki, W. J., Crepp, J. R., Everett, M. E., Horch, E. P., Howard, A. W., Kolbl, R., Marcy, G. W., McCauliff, S., & Quintana, E. V. 2015, ApJ, 800, 99

van Dam, M. A., Bouchez, A. H., Le Mignant, D., Johansson, E. M., Wizinowich, P. L., Campbell, R. D., Chin, J. C. Y., Hartman, S. K., Lafon, R. E., Stomski, Jr., P. J., & Summers, D. M. 2006, PASP, 118, 310

Wang, J., Fischer, D. A., Horch, E. P., & Xie, J.-W. 2015a, ApJ, 806, 248

Wang, J., Fischer, D. A., Xie, J.-W., & Ciardi, D. R. 2014a, ApJ, 791, 111

—. 2015b, ApJ, 813, 130

Wang, J., Xie, J.-W., Barclay, T., & Fischer, D. A. 2014b, ApJ, 783, 4

Wizinowich, P. L., Le Mignant, D., Bouchez, A. H., Campbell, R. D., Chin, J. C. Y., Contos, A. R., van Dam, M. A., Hartman, S. K., Johansson, E. M., Lafon, R. E., Lewis, H., Stomski, P. J., Summers, D. M., Brown, C. G., Danforth, P. M., Max, C. E., & Pennington, D. M. 2006, PASP, 118, 297

Yelda, S., Lu, J. R., Ghez, A. M., Clarkson, W., Anderson, J., Do, T., & Matthews, K. 2010, ApJ, 725, 331

York, D. G., Adelman, J., Anderson, Jr., J. E., Anderson, S. F., Annis, J., Bahcall, N. A., Bakken, J. A., Barkhouser, R., Bastian, S., Berman, E., Boroski, W. N., Bracker, S., Briegel, C., Briggs, J. W., Brinkmann, J., Brunner, R., Burles, S., Carey, L., Carr, M. A., Castander, F. J., Chen, B., Colestock, P. L., Connolly, A. J., Crocker, J. H., Csabai, I., Czarapata, P. C., Davis, J. E., Doi, M., Dombeck, T., Eisenstein, D., Ellman, N., Elms, B. R., Evans, M. L., Fan, X., Federwitz, G. R., Fiscelli, L., Friedman, S., Frieman, J. A., Fukugita, M., Gillespie, B., Gunn, J. E., Gurbani, V. K., de Haas, E., Haldeman, M., Harris, F. H., Hayes, J., Heckman, T. M., Hennessy, G. S., Hindsley, R. B., Holm, S., Holmgren, D. J., Huang, C.-h., Hull, C., Husby, D., Ichikawa, S.-I., Ichikawa, T., Ivezić, Ž., Kent, S., Kim, R. S. J., Kinney, E., Klaene, M., Kleinman, A. N., Kleinman, S., Knapp, G. R., Korienek, J., Kron, R. G., Kunszt, P. Z., Lamb, D. Q., Lee, B., Leger, R. F., Limmongkol, S., Lindenmeyer, C., Long, D. C., Loomis, C., Loveday, J., Lucinio, R., Lupton, R. H., MacKinnon, B., Mannery, E. J., Mantsch, P. M., Margon, B., McGehee, P., McKay, T. A., Meiksin, A., Merelli, A., Monet, D. G., Munn, J. A., Narayanan, V. K., Nash, T., Neilsen, E., Neswold, R., Newberg, H. J., Nichol, R. C., Nicinski, T., Nonino, M., Okada, N., Okamura, S., Ostriker, J. P., Owen, R., Pauls, A. G., Peoples, J., Peterson, R. L., Petravick, D., Pier, J. R., Pope, A., Pordes, R., Prosapio, A., Rechenmacher, R., Quinn, T. R., Richards, G. T., Richmond, M. W., Rivetta, C. H., Rockosi, C. M., Ruthmansdorfer, K., Sandford, D., Schlegel, D. J., Schneider, D. P., Sekiguchi, M., Sergey, G., Shimasaku, K., Siegmund, W. A., Smee, S., Smith, J. A., Snedden, S., Stone, R., Stoughton, C., Strauss, M. A., Stubbs, C., SubbaRao, M., Szalay, A. S., Szapudi, I., Szokoly, G. P., Thakar, A. R., Tremonti, C., Tucker, D. L., Uomoto, A., Vanden Berk, D., Vogeley, M. S., Waddell, P., Wang, S.-i., Watanabe, M., Weinberg, D. H., Yanny, B., Yasuda, N., & SDSS Collaboration. 2000, AJ, 120, 1579

Table 2
Detections of Objects within ∼4.″0 of *Kepler* Planet Candidates at ≥ 5σ Significance

KOI	m_i (mag)	ObsID	Filter	Signf. σ	Separation (arcsec)	P.A. (deg.)	Mag. Diff. (mag)	Previous Detection?	NIRC2 Detection?
KOI-4	11.3	2012/07/16	i'	12	3.42±0.06	75±2	4.46±0.05		
KOI-42	9.2	2013/07/28	LP600	35	1.74±0.06	35±2	3.04±0.17	A12, H11, K16	
KOI-227	13.7	2013/07/27	LP600	5	0.33±0.06	72±6	0.84±0.09	H11, K16	
KOI-258	9.8	2012/07/18	i'	14	1.05±0.06	77±2	2.76±0.17	A12, H11	
KOI-284	11.7	2013/07/27	LP600	19	0.96±0.06	98±2	0.45±0.04	A12, H11, E15, K16	
KOI-298	12.4	2013/08/15	LP600	477	2.11±0.06	270±2	0.58±0.04	LB12, K16	
KOI-379	13.2	2013/07/27	LP600	56	2.11±0.06	83±2	1.42±0.11	LB12	
KOI-521	14.5	2013/08/14	LP600	18	3.24±0.06	152±2	0.42±0.03		
KOI-558	14.6	2013/08/22	LP600	6	3.16±0.06	271±2	2.06±0.04		
KOI-641	13.1	2013/07/24	LP600	18	2.09±0.06	278±2	2.07±0.05	LB12	
				46	3.65±0.06	205±2	0.33±0.06	LB12	
KOI-645	13.5	2013/07/25	LP600	6	2.98±0.06	48±2	2.23±0.04	LB12	
KOI-652	13.3	2013/07/28	LP600	21	1.23±0.06	272±2	1.59±0.14	K15, K16, Te15	
KOI-697	13.5	2013/08/15	LP600	9	0.71±0.06	54±3	0.06±0.03	W15	
KOI-801	14.8	2013/10/25	LP600	6	3.67±0.06	195±2	2.58±0.11		
KOI-976		2012/08/03	i'	22	0.25±0.06	129±7	0.34±0.09	K16	
KOI-1061	14.3	2013/08/20	LP600	14	1.22±0.06	38±2	1.21±0.07		
KOI-1300	13.9	2013/08/16	LP600	8	0.78±0.06	357±3	1.79±0.18	K16	
KOI-1357	15.3	2013/08/18	LP600	30	3.83±0.06	167±2	3.38±0.03		
KOI-1531	12.9	2013/08/16	LP600	7	0.43±0.06	99±4	0.90±0.16		
KOI-1546	14.2	2013/08/19	LP600	6	0.62±0.06	86±3	1.03±0.12	LB14	yes
KOI-1717	14.3	2013/10/25	LP600	9	0.87±0.06	305±3	1.46±0.13		
KOI-1853	13.3	2013/08/14	LP600	11	0.96±0.06	304±2	0.24±0.05		
KOI-1861	13.8	2013/07/28	LP600	5	2.10±0.06	84±2	4.93±0.16		
KOI-1899	14.4	2013/07/27	LP600	16	1.84±0.06	342±2	0.94±0.05		
KOI-1972	13.6	2013/08/15	LP600	21	1.05±0.06	246±2	1.05±0.12		
KOI-2032	12.0	2013/07/28	LP600	17	1.19±0.06	317±2	0.34±0.05	K16	
KOI-2067	12.3	2013/07/24	LP600	17	1.64±0.06	315±2	0.80±0.04	K16	
KOI-2096	14.9	2013/08/19	LP600	29	3.50±0.06	17±2	4.13±0.11		
KOI-2098	13.7	2013/07/27	LP600	8	2.88±0.06	156±2	2.58±0.04		
				10	3.24±0.06	132±2	2.40±0.06		
KOI-2100	14.4	2013/07/28	LP600	8	2.98±0.06	318±2	2.10±0.05		
KOI-2174	15.2	2012/08/07	LP600	10	0.92±0.06	226±2	0.21±0.06		
				25	3.88±0.06	314±2	0.14±0.03		
KOI-2295	11.4	2013/07/29	LP600	21	2.19±0.06	78±2	0.88±0.06	K16	
KOI-2298	13.5	2013/08/16	LP600	29	1.57±0.06	194±2	2.08±0.14	D14	
KOI-2377	14.5	2013/07/24	LP600	14	2.09±0.06	335±2	1.25±0.03		yes
KOI-2421	14.0	2013/07/25	LP600	8	1.23±0.06	290±2	0.99±0.09	D14	
KOI-2474	13.9	2013/08/13	LP600	8	0.61±0.06	279±3	0.65±0.07	H12	
KOI-2598	14.0	2013/08/13	LP600	9	1.09±0.06	75±2	0.37±0.04		
KOI-2601	13.8	2013/08/13	LP600	17	1.66±0.06	14±2	1.43±0.06		
KOI-2679	13.3	2013/07/25	LP600	19	2.11±0.06	324±2	2.87±0.06		
KOI-2705	14.3	2013/07/25	LP600	15	1.84±0.06	304±2	3.19±0.14	G16, K16	yes
KOI-2711	13.5	2013/07/29	LP600	8	0.52±0.06	147±4	0.12±0.08		yes
KOI-2729	13.7	2013/08/18	LP600	6	3.94±0.06	278±2	2.03±0.12		
KOI-2754		2013/08/14	LP600	21	0.79±0.06	260±3	2.23±0.20	D14, K16	
KOI-2771		2013/08/16	LP600	13	3.85±0.06	312±2	6.61±0.14	D14	
KOI-2803	12.1	2013/08/13	LP600	25	3.84±0.06	61±2	3.00±0.05	D14, K16	
KOI-2807	13.7	2013/07/28	LP600	13	3.93±0.06	77±2	1.90±0.04		
KOI-2812	14.2	2013/07/27	LP600	22	2.09±0.06	335±2	3.23±0.05		
KOI-2836	14.9	2013/10/22	LP600	217	3.94±0.06	70±2	3.39±0.04		
KOI-2837	13.1	2013/08/15	LP600	6	0.35±0.06	136±5	0.23±0.04		yes
KOI-2848	12.3	2013/08/14	LP600	6	2.30±0.06	28±2	5.63±0.23		
KOI-2904	12.5	2013/07/24	LP600	10	0.71±0.06	226±3	1.99±0.24	D14	yes
KOI-2910	15.0	2013/08/19	LP600	7	3.15±0.06	88±2	0.72±0.05		
KOI-2962	14.0	2013/07/25	LP600	9	1.13±0.06	68±2	0.53±0.05		
KOI-3069	14.7	2013/08/19	LP600	5	1.93±0.06	109±2	2.20±0.07		yes
KOI-3073	14.2	2013/08/14	LP600	10	1.30±0.06	10±2	1.76±0.15		
KOI-3158		2013/07/21	LP600	613	2.10±0.06	254±2	4.00±0.15	LB14, K16, C15	
KOI-3190	11.1	2013/07/27	LP600	6	2.68±0.06	190±2	5.92±0.17		
KOI-3245	12.3	2013/07/25	LP600	12	1.58±0.06	184±2	3.10±0.07		
KOI-3324	15.7	2013/10/23	LP600	11	3.84±0.06	323±2	3.05±0.06		
KOI-3339	14.4	2013/10/22	LP600	9	3.41±0.06	346±2	1.38±0.06		
KOI-3468	14.1	2013/07/24	LP600	6	1.49±0.06	117±2	3.22±0.15		
KOI-3497	13.0	2013/10/24	LP600	15	0.78±0.06	174±3	1.23±0.12	M14, K16	
KOI-3891	13.4	2013/07/27	LP600	5	1.05±0.06	240±2	4.69±0.41	K16	
				9	2.01±0.06	136±2	4.92±0.13	K16	
KOI-3907	12.5	2013/07/27	LP600	7	1.58±0.06	162±2	6.31±0.25	W15	
				20	2.82±0.06	72±2	3.23±0.04	W15	
KOI-4004	12.5	2013/07/27	LP600	13	1.93±0.06	217±2	4.34±0.27	K16	yes
KOI-4021	12.5	2013/08/16	LP600	11	1.92±0.06	113±2	0.52±0.07		

Table 2 — *Continued*

KOI	m_i (mag)	ObsID	Filter	Signf. σ	Separation (arcsec)	P.A. (deg.)	Mag. Diff. (mag)	Previous Detection?	NIRC2 Detection?
KOI-4145	14.1	2013/07/27	LP600	9	2.71±0.06	237±2	2.36±0.03		
KOI-4149	14.1	2013/10/22	LP600	11	1.76±0.06	63±2	0.17±0.03		
KOI-4205	14.2	2013/07/28	LP600	7	2.71±0.06	66±2	2.65±0.03		
KOI-4209	15.7	2013/08/19	LP600	11	0.96±0.06	203±2	0.37±0.08		yes
KOI-4287	11.1	2013/08/17	LP600	10	0.61±0.06	76±3	1.27±0.14	K16	
KOI-4329	11.9	2013/08/18	LP600	10	1.93±0.06	117±2	4.64±0.21		
KOI-4331	13.0	2013/07/29	LP600	6	0.45±0.06	103±4	0.25±0.04		yes
KOI-4389	14.8	2013/08/21	LP600	7	2.88±0.06	332±2	0.58±0.06		
KOI-4399	11.8	2013/07/24	LP600	6	2.16±0.06	17±2	6.24±0.21	K16	
KOI-4407	11.0	2013/07/24	LP600	19	2.54±0.06	298±2	2.97±0.05	E15, K16	yes
KOI-4463	14.6	2013/07/27	LP600	29	2.45±0.06	143±2	0.01±0.03		yes
KOI-4495	15.2	2013/08/22	LP600	6	3.06±0.06	89±2	3.90±0.06		
				9	3.41±0.06	344±2	2.68±0.05		
KOI-4567	13.6	2013/07/24	LP600	12	1.31±0.06	142±2	2.48±0.13		
KOI-4575	13.0	2013/08/16	LP600	18	2.97±0.06	61±2	2.18±0.03		
KOI-4580	12.8	2013/08/13	LP600	19	1.58±0.06	60±2	1.27±0.05		
KOI-4582	11.6	2013/07/27	LP600	68	2.71±0.06	308±2	6.28±0.18	K16	
				39	3.55±0.06	286±2	3.27±0.12	K16	
KOI-4634	13.5	2013/07/24	LP600	5	0.35±0.06	275±5	1.55±0.18		yes
KOI-4651	13.6	2013/07/25	LP600	9	1.22±0.06	105±2	2.88±0.37		
KOI-4656	13.7	2013/07/29	LP600	8	2.89±0.06	23±2	1.42±0.03		
KOI-4657	13.0	2013/07/29	LP600	22	2.11±0.06	234±2	3.27±0.10	K16	
KOI-4792	14.0	2013/08/15	LP600	9	3.68±0.06	318±2	2.36±0.04		
KOI-4797	15.3	2013/08/22	LP600	6	3.59±0.06	127±2	1.12±0.06		
KOI-4813	13.3	2013/07/28	LP600	5	2.54±0.06	208±2	1.22±0.05		
KOI-4823	12.5	2013/08/17	LP600	16	1.40±0.06	153±2	0.59±0.04		
KOI-4871	12.9	2013/10/25	LP600	11	0.96±0.06	333±2	3.12±0.19	[a]	yes

Notes: References for previous detections are denoted with the following codes: Adams et al. 2012 (A12); Campante et al. 2015 (C15); Dressing et al. 2014 (D14); Everett et al. 2015 (E15); Gaidos et al. 2016 (G16); Howell et al. 2011 (H11); Horch et al. 2012 (H12); Kraus et al. 2016 (K16); Lillo-Box et al. 2012 (LB12); Lillo-Box et al. 2014 (LB14); Muirhead et al. 2014 (M14); Teske et al. 2015 (Te15); Wang et al. 2015b (W15).

[a] Companion identity is ambiguous. See Section 5.2.

Table 3
Detections of Objects within ∼4.″0 of *Kepler* Planet Candidates at $< 5\sigma$ Significance

KOI	m_i (mag)	ObsID	Filter	Signf. σ	Separation (arcsec)	P.A. (deg.)	Mag. Diff. (mag)	Previous Detection?	NIRC2 Detection?
KOI-151	13.8	2013/07/27	LP600	4.2	4.17±0.06	58±2	5.84±0.18		
KOI-155	13.3	2013/08/13	LP600	4.0	4.01±0.06	251±2	3.83±0.17		
KOI-190	13.9	2013/07/27	LP600	3.6	0.23±0.06	105±2	1.33±0.18		yes
KOI-251	14.1	2013/08/21	LP600	2.1	3.48±0.06	123±2	3.80±0.12	A12, G16, K16	
KOI-285		2013/08/13	LP600	4.6	1.51±0.06	136±2	6.12±0.21	A12, K16	
KOI-387	13.2	2013/07/29	LP600	2.3	0.98±0.06	352±2	3.86±0.18	LB12, K16	
KOI-425	14.5	2013/08/22	LP600	2.8	0.53±0.06	346±4	0.86±0.10		yes
KOI-438	13.8	2013/08/18	LP600	3.9	3.28±0.06	181±2	3.11±0.04	K16	
KOI-507	14.6	2013/08/22	LP600	2.3	2.03±0.06	358±2	4.46±0.11		
KOI-584	13.9	2012/08/05	LP600	2.5	1.83±0.06	137±2	4.10±0.12		
KOI-592	14.1	2013/08/14	LP600	2.6	2.30±0.06	150±2	4.21±0.11	LB12	
KOI-614	14.3	2013/07/29	LP600	2.2	2.76±0.06	214±2	4.01±0.03		
KOI-730	15.1	2013/08/21	LP600	3.8	2.04±0.06	237±2	2.95±0.09		
KOI-813	15.5	2013/08/22	LP600	4.3	3.87±0.06	137±2	2.09±0.08		
KOI-931	15.0	2013/10/23	LP600	4.0	1.38±0.06	177±2	3.40±0.14		yes
KOI-999	15.0	2013/08/18	LP600	2.6	3.41±0.06	125±2	2.80±0.05		
KOI-1066	15.4	2013/08/21	LP600	2.2	1.69±0.06	205±2	4.19±0.18		yes
KOI-1067	14.5	2013/10/23	LP600	3.5	2.97±0.06	143±2	4.05±0.15		yes
KOI-1112	14.4	2013/07/27	LP600	2.5	2.95±0.06	172±2	4.57±0.05		yes
KOI-1214	14.4	2013/07/24	LP600	3.9	0.33±0.06	132±2	1.21±0.18		yes
KOI-1397	14.8	2013/08/21	LP600	3.1	2.30±0.06	229±2	4.41±0.17	K16	
KOI-1495	15.2	2013/08/22	LP600	2.5	3.75±0.06	188±2	2.92±0.11		
KOI-1546	14.2	2013/08/19	LP600	4.2	4.15±0.06	165±2	3.34±0.07	LB14	yes
				3.5	2.93±0.06	5±2	3.52±0.08	LB14	yes
KOI-1573	14.2	2013/07/25	LP600	3.7	3.84±0.06	299±2	4.72±0.15		
KOI-1599	14.6	2013/08/18	LP600	3.4	2.98±0.06	207±2	2.22±0.06		
				2.6	3.42±0.06	316±2	2.89±0.05		
KOI-1700	14.1	2013/07/27	LP600	3.6	0.29±0.06	289±2	1.07±0.26		yes
KOI-1784	13.4	2013/07/28	LP600	4.7	0.33±0.06	286±6	0.58±0.13	K15, W15	yes
KOI-1798	14.2	2013/08/13	LP600	2.4	3.81±0.06	186±2	3.75±0.21		
KOI-1830	14.2	2013/07/27	LP600	3.9	0.46±0.06	319±4	1.29±0.17		
KOI-1950	15.7	2013/08/22	LP600	3.6	3.35±0.06	326±2	1.69±0.05		
KOI-1985	13.4	2013/07/24	LP600	2.2	2.82±0.06	156±2	4.19±0.09	K16	
KOI-1989	13.1	2013/08/14	LP600	2.9	1.12±0.06	41±2	3.49±0.16		yes
KOI-2014	15.4	2013/10/23	LP600	3.1	3.75±0.06	267±2	2.50±0.04		
KOI-2019	15.4	2013/08/22	LP600	3.3	4.01±0.06	105±2	2.61±0.21		
KOI-2055	14.3	2013/07/25	LP600	2.2	3.80±0.06	57±2	4.09±0.05		
KOI-2056	14.3	2013/08/16	LP600	4.9	3.87±0.06	131±2	3.37±0.11		
KOI-2069	13.6	2013/08/14	LP600	2.7	1.12±0.06	108±2	4.24±0.51		
KOI-2083	13.4	2013/07/28	LP600	2.5	0.26±0.06	176±2	1.03±0.18		yes
KOI-2115	15.8	2013/07/21	LP600	2.4	3.59±0.06	243±2	2.75±0.12		
KOI-2156	15.3	2013/08/18	LP600	2.0	3.35±0.06	303±2	2.64±0.05	G16, K16	
KOI-2247	14.0	2013/07/27	LP600	2.3	1.90±0.06	355±2	5.12±0.21		
KOI-2314	14.4	2013/07/27	LP600	4.6	4.14±0.06	201±2	3.45±0.22		
KOI-2317	14.1	2013/07/27	LP600	4.6	1.51±0.06	110±2	4.93±0.19		yes
KOI-2377	14.5	2013/07/24	LP600	4.3	4.11±0.06	326±2	4.04±0.12		yes
KOI-2380	14.0	2013/07/24	LP600	4.0	4.01±0.06	250±2	2.46±0.08		
KOI-2421	14.0	2013/07/25	LP600	4.1	4.07±0.06	132±2	3.87±0.18	D14	
KOI-2469	14.7	2013/08/18	LP600	3.8	4.18±0.06	114±2	2.44±0.17		
KOI-2493	15.0	2013/08/22	LP600	2.4	2.69±0.06	300±2	2.68±0.04		
KOI-2516	13.1	2013/07/27	LP600	4.0	3.42±0.06	84±2	5.93±0.04	D14	
KOI-2542	14.8	2013/08/21	LP600	3.4	0.88±0.06	22±3	1.20±0.19	G16, K16	yes
KOI-2551	15.5	2013/10/23	LP600	3.5	2.69±0.06	197±2	1.93±0.03		
KOI-2601	13.8	2013/08/13	LP600	3.8	1.44±0.06	297±2	3.61±0.14		
KOI-2664	15.3	2013/08/18	LP600	4.4	1.17±0.06	90±2	0.83±0.09		yes
KOI-2681	15.7	2013/10/23	LP600	4.2	1.10±0.06	161±2	1.25±0.11		yes
KOI-2707	14.2	2013/07/24	LP600	2.2	3.28±0.06	217±2	4.71±0.16		
				2.9	3.87±0.06	182±2	3.64±0.11		
KOI-2722	13.1	2013/08/14	LP600	3.7	3.27±0.06	282±2	5.88±0.14	D14	yes
KOI-2743	13.5	2013/08/14	LP600	3.1	2.36±0.06	182±2	3.79±0.08		
KOI-2779	14.8	2013/10/22	LP600	2.9	0.98±0.06	61±2	2.54±0.38		
KOI-2838	13.2	2013/08/13	LP600	2.4	1.74±0.06	197±2	5.92±0.35	D14	
KOI-2859	13.6	2013/08/16	LP600	3.1	0.47±0.06	282±5	2.12±0.23		yes
KOI-2914	12.1	2013/07/24	LP600	2.4	3.80±0.06	231±2	5.64±0.06	D14	
KOI-2949	13.1	2013/07/29	LP600	2.2	2.36±0.06	311±2	4.08±0.32		
KOI-2971	12.6	2013/07/24	LP600	3.9	0.53±0.06	209±4	1.33±0.18		yes
KOI-2984	12.9	2013/07/24	LP600	4.1	3.47±0.06	33±2	4.34±0.05	D14	
KOI-3029	14.7	2013/08/18	LP600	3.1	0.28±0.06	272±2	0.68±0.22		yes
KOI-3041	14.0	2013/07/25	LP600	3.2	2.03±0.06	128±2	4.64±0.17		
KOI-3255	13.9	2013/07/27	LP600	2.2	3.15±0.06	44±2	4.87±0.05	E15, K16	
KOI-3277	12.9	2013/07/24	LP600	2.1	2.45±0.06	355±2	5.79±0.23		

Table 3 — *Continued*

KOI	m_i (mag)	ObsID	Filter	Signf. σ	Separation (arcsec)	P.A. (deg.)	Mag. Diff. (mag)	Previous Detection?	NIRC2 Detection?
				3.8	3.41±0.06	353±2	5.00±0.12		
KOI-3284	13.8	2013/08/22	LP600	4.2	3.94±0.06	4±2	2.42±0.08	To15, E15, G16, K16	
KOI-3288	14.0	2013/07/24	LP600	2.4	3.17±0.06	75±2	4.32±0.12		
				2.1	3.50±0.06	80±2	4.62±0.16		
KOI-3309	14.4	2013/08/17	LP600	3.2	3.71±0.06	42±2	2.78±0.04	K16	
KOI-3377	14.9	2013/08/22	LP600	2.7	1.45±0.06	58±2	4.26±0.19		yes
KOI-3401	14.2	2013/07/28	LP600	4.3	0.65±0.06	94±3	0.89±0.20		
KOI-3439	14.0	2013/07/24	LP600	2.8	3.42±0.06	228±2	3.97±0.05		
KOI-3444	13.0	2013/07/25	LP600	2.6	1.11±0.06	8±2	3.32±0.17	LB14, W15, G16, K16	
				3.2	3.55±0.06	262±2	3.41±0.23	LB14, W15, G16, K16	
KOI-3459	15.0	2013/08/21	LP600	3.3	3.35±0.06	124±2	2.37±0.04		
KOI-3460	14.3	2013/07/27	LP600	2.5	1.24±0.06	153±2	5.08±0.13		
				2.8	2.47±0.06	231±2	5.52±0.11		
KOI-3486	14.1	2013/07/24	LP600	2.7	4.16±0.06	260±2	4.06±0.12		
KOI-3500	13.0	2013/07/25	LP600	4.1	2.54±0.06	137±2	4.01±0.05		
KOI-3946	13.1	2013/08/13	LP600	3.9	4.27±0.06	61±2	5.26±0.13		
KOI-4053	12.6	2013/07/25	LP600	3.2	4.11±0.06	302±2	5.51±0.12		
KOI-4098	13.5	2013/08/15	LP600	4.5	0.78±0.06	174±3	1.10±0.22		
KOI-4166	15.0	2013/08/18	LP600	2.0	3.54±0.06	157±2	3.29±0.04		
KOI-4194	15.0	2013/08/21	LP600	2.3	2.17±0.06	290±2	3.41±0.07		
KOI-4208	15.3	2013/08/17	LP600	3.3	0.99±0.06	234±2	2.57±0.29		
KOI-4226	12.6	2013/07/24	LP600	4.7	2.49±0.06	267±2	4.18±0.03	K16	
KOI-4274	15.1	2013/08/22	LP600	3.1	3.26±0.06	207±2	3.71±0.11		
				2.4	4.54±0.06	327±2	4.11±0.13		
KOI-4313	14.1	2013/08/13	LP600	2.6	2.88±0.06	81±2	4.19±0.05		
KOI-4409	12.3	2013/07/24	LP600	2.3	2.89±0.06	139±2	6.10±0.10		
KOI-4443	13.7	2013/08/13	LP600	2.2	3.41±0.06	26±2	5.00±0.13		
KOI-4495	15.2	2013/08/22	LP600	3.9	3.04±0.06	58±2	4.73±0.09		
KOI-4523	14.6	2013/08/21	LP600	2.4	3.94±0.06	100±2	2.61±0.33		
KOI-4699	12.8	2013/08/13	LP600	2.8	4.01±0.06	285±2	5.93±0.21		
KOI-4768	15.4	2013/10/23	LP600	2.3	1.30±0.06	159±2	3.99±0.26		yes
KOI-4797	15.3	2013/08/22	LP600	3.5	3.93±0.06	77±2	3.37±0.11		
KOI-4812	15.5	2013/10/23	LP600	3.6	3.15±0.06	100±2	1.84±0.03		
KOI-4813	13.3	2013/07/28	LP600	4.6	4.03±0.06	146±2	3.34±0.09		

Notes: References for previous detections are denoted with the following codes: Adams et al. 2012 (A12); Dressing et al. 2014 (D14); Everett et al. 2015 (E15); Gaidos et al. 2016 (G16); Kolbl et al. 2015 (K15); Kraus et al. 2016 (K16); Lillo-Box et al. 2012 (LB12); Lillo-Box et al. 2014 (LB14); Torres et al. 2015 (To15); Wang et al. 2015b (W15).

Table 4
Full Keck-NIRC2 Observation List and Detected Companions

KOI	ObsID	Filter	Separation (arcsec)	P.A. (deg.)	Mag. Diff. (mag)	Notes
KOI-190	2015 Jul 25	Kp	0.180±0.010	109±3	0.64±0.14	Table 3
KOI-425	2015 Jul 25	Kp	0.490±0.010	343±1	0.83±0.06	Table 3
KOI-628	2013 Aug 25	Kp	1.828±0.005	311±1	3.87±0.06	PI
			2.752±0.005	239±1	3.00±0.06	c
KOI-931	2015 Jul 25	Kp	1.261±0.005	177±1	3.23±0.06	Table 3
KOI-987	2013 Aug 25	Kp	1.977±0.005	226±1	2.24±0.06	PI
KOI-1066	2014 Aug 17	Kp	1.687±0.005	231±1	2.95±0.07	Table 3
KOI-1067	2014 Aug 17	Kp	2.923±0.005	142±1	3.79±0.11	Table 3
KOI-1112	2013 Aug 24	Kp	3.063±0.005	172±1	2.76±0.07	Table 3
KOI-1151	2014 Aug 17	Kp	0.756±0.010	307±1	2.41±0.06	PI
KOI-1214	2014 Aug 17	Kp	0.347±0.010	136±2	2.46±0.06	Table 3
KOI-1359	2013 Jun 25	Ks	1.387±0.005	332±1	2.17±0.06	PI
KOI-1375	2014 Aug 17	Kp	0.785±0.010	27±1	3.39±0.07	PI
KOI-1442	2013 Aug 25	Kp	2.113±0.005	71±1	3.63±0.06	PI
KOI-1546	2013 Aug 24	Kp	0.600±0.010	90±1	0.73±0.05	Table 2
			2.918±0.005	4±1	2.95±0.08	Table 3
			4.108±0.005	165±1	3.48±0.06	Table 3
KOI-1700	2014 Aug 17	Kp	0.274±0.010	288±2	0.55±0.06	Table 3
KOI-1784	2015 Jul 25	Kp	0.279±0.010	291±2	0.78±0.06	Table 3
KOI-1845	2013 Jun 25	Ks	1.996±0.005	79±1	2.89±0.06	PI
			2.963±0.005	348±1	4.40±0.09	c
KOI-1884	2013 Aug 24	K	0.934±0.010	95±1	2.31±0.06	PI
			1.838±0.005	82±1	2.73±0.06	b
			2.567±0.005	327±1	3.20±0.14	b
KOI-1891	2013 Aug 24	Kp	2.069±0.005	211±1	4.60±0.07	PI
KOI-1989	2015 Jul 25	Kp	0.817±0.010	40±1	2.92±0.06	Table 3
KOI-2009	2013 Aug 25	Kp	1.511±0.005	178±1	2.75±0.06	PI
KOI-2083	2014 Aug 17	Kp	0.252±0.010	166±1	1.60±0.05	Table 3
KOI-2159	2014 Aug 17	Kp	2.018±0.005	324±1	2.48±0.06	PI
KOI-2317	2015 Jul 25	Kp	1.512±0.005	112±1	3.92±0.06	Table 3
KOI-2363	2014 Aug 17	Kp	1.952±0.005	357±1	5.04±0.09	b
KOI-2377	2013 Aug 24	Kp	2.186±0.005	335±1	0.63±0.07	Table 2
			2.544±0.005	42±1	3.75±0.12	b
			3.911±0.005	316±1	3.55±0.17	Table 3
KOI-2413	2013 Aug 25	Kp	0.308±0.010	250±2	0.17±0.06	PI
KOI-2443	2013 Jun 25	Ks	1.383±0.005	164±1	3.63±0.06	PI
KOI-2542	2015 Jul 25	Kp	0.765±0.010	29±1	0.60±0.05	Table 3
KOI-2664	2015 Jul 25	Kp	1.180±0.005	90±1	1.10±0.06	Table 3
KOI-2681	2014 Aug 17	Kp	1.132±0.005	148±1	0.43±0.06	Table 3
KOI-2705	2013 Aug 24	Kp	1.900±0.005	304±1	2.58±0.07	Table 2
KOI-2711	2014 Aug 17	Kp	0.466±0.010	149±1	0.12±0.06	Table 2
KOI-2722	2014 Aug 17	Kp	3.226±0.005	283±1	3.77±0.06	Table 3
KOI-2837	2013 Aug 24	Kp	0.347±0.010	138±2	0.20±0.06	Table 2
KOI-2859	2014 Aug 17	Kp	0.454±0.010	291±1	2.89±0.06	Table 3
KOI-2904	2013 Aug 24	Kp	0.700±0.010	226±1	2.45±0.06	Table 2
KOI-2971	2015 Jul 25	Kp	0.301±0.010	274±2	3.57±0.06	Table 3
			3.564±0.005	38±1	5.93±0.17	b
KOI-3029	2014 Aug 17	Kp	0.251±0.010	264±2	0.06±0.06	Table 3
			1.734±0.005	356±1	4.49±0.07	b
			2.552±0.005	4±1	3.44±0.07	b
KOI-3069	2013 Aug 24	Kp	1.785±0.005	108±1	1.26±0.06	Table 2
KOI-3377	2015 Jul 25	Kp	0.264±0.010	335±2	0.49±0.06	b
			1.405±0.005	50±1	3.74±0.06	Table 3
KOI-4004	2015 Jul 25	Kp	1.958±0.005	218±1	2.37±0.08	Table 2
KOI-4209	2013 Aug 24	Kp	0.975±0.010	205±1	0.57±0.06	Table 2
KOI-4292	2013 Aug 25	Kp	1.951±0.005	30±1	4.54±0.08	b
KOI-4331	2014 Aug 17	Kp	0.347±0.010	102±2	0.13±0.05	Table 2
KOI-4407	2013 Aug 25	Kp	2.455±0.005	300±1	1.89±0.06	Table 2
			2.662±0.005	311±1	4.65±0.34	b
KOI-4463	2013 Aug 24	Kp	2.462±0.005	144±1	-0.26±0.07	Table 2
KOI-4634	2015 Jul 25	Kp	0.282±0.010	276±2	0.65±0.06	Table 2
KOI-4768	2014 Aug 17	Kp	1.326±0.005	160±1	2.61±0.07	Table 3
KOI-4871	2014 Aug 17	Kp	0.921±0.010	334±1	3.04±0.06	Table 2

[a]PI = Confirmation of $< 5\sigma$ significance companions in Paper I.
[b]Companion not detected in Robo-AO image.
[c]Additional detection not reported in Paper I. (Angular separation exceeds $2\farcs5$.)

Table 5
Full Robo-AO Observation List

KOI	m_i/mags	ObsID	Obs. qual.*	Companion?
K00004.01	11.3	2012/07/16	high (i'-band)	yes
K00042.01	9.2	2013/07/28	high	yes
K00116.01	12.7	2013/07/24	high	
K00123.01	12.2	2013/07/25	high	
K00127.01	13.7	2013/08/15	high	
K00138.01	13.9	2013/07/29	medium	
K00150.01	13.6	2013/07/27	high	
K00151.01	13.8	2013/07/27	high	yes
K00155.01	13.3	2013/08/13	high	yes
K00183.01	14.1	2013/08/15	medium	
K00188.01	14.5	2013/08/22	medium	
K00189.01	14.1	2013/08/17	medium	
K00190.01	13.9	2013/07/27	medium	yes
K00192.01	14.1	2013/08/15	medium	
K00202.01	14.1	2013/08/13	low	
K00205.01	14.2	2013/07/27	high	
K00206.01	14.3	2013/07/25	medium	
K00208.01	14.8	2013/08/21	low	
K00221.01	14.4	2013/07/27	medium	
K00227.01	13.7	2013/07/27	low	yes
K00234.01	14.1	2013/08/15	medium	
K00235.01	14.1	2013/07/29	medium	
K00239.01	14.6	2013/08/22	medium	
K00245.01		2013/07/28	high	
K00251.01	14.1	2013/08/21	medium	yes
K00257.01	10.7	2013/07/27	high	
K00258.01	9.8	2012/07/18	high (i'-band)	yes
K00262.01	10.3	2012/07/28	high (i'-band)	
K00265.01	11.9	2013/08/13	high	
K00271.01	11.4	2012/08/02	high (i'-band)	
K00274.01	11.3	2013/07/28	high	
K00284.01	11.7	2013/07/27	medium	yes
K00285.01		2013/08/13	medium	yes
K00289.01	12.5	2013/08/13	high	
K00292.01	12.7	2013/08/18	low	
K00295.01	12.2	2013/08/17	high	
K00298.01	12.4	2013/08/15	high	yes
K00304.01	12.4	2013/07/29	high	
K00318.01	12.1	2013/08/15	high	
K00326.01	13.0	2013/07/29	high	
K00338.01	13.1	2013/07/28	high	
K00346.01	13.2	2013/07/27	high	
K00351.01	13.7	2013/08/15	medium	
K00354.01	13.1	2013/08/15	high	
K00355.01	13.0	2013/08/15	high	
K00367.01	10.9	2013/07/27	high	
K00369.01	11.9	2013/07/24	high	
K00370.01	11.8	2013/08/14	medium	
K00374.01	12.0	2013/08/15	high	
K00375.01	13.1	2013/08/17	high	
K00379.01	13.2	2013/07/27	high	yes
K00387.01	13.2	2013/07/29	medium	yes
K00410.01	14.3	2013/07/29	medium	
K00412.01	14.1	2013/07/25	low	
K00417.01	14.6	2013/10/22	low	
K00419.01	14.3	2013/08/13	medium	
K00420.01	13.9	2013/08/13	high	
K00421.01	14.7	2013/08/21	low	
K00425.01	14.5	2013/08/22	low	yes
K00429.01	14.2	2013/07/28	medium	
K00432.01	14.1	2013/08/17	medium	
K00433.01	14.6	2013/08/21	low	
K00438.01	13.8	2013/08/18	medium	yes
K00443.01	14.0	2013/07/24	medium	
K00446.01	14.0	2013/07/27	medium	
K00448.01	14.5	2013/08/22	medium	
K00460.01	14.5	2013/10/23	medium	
K00470.01	14.5	2013/10/23	medium	
K00473.01	14.4	2013/10/22	low	
K00475.01	14.5	2012/09/01	medium	
K00477.01	14.4	2013/08/22	low	
K00480.01	14.1	2013/08/17	medium	
K00484.01	14.2	2013/08/17	medium	
K00487.01	14.3	2013/08/18	medium	

Table 5 — *Continued*

KOI	m_i/mags	ObsID	Obs. qual.*	Companion?
K00488.01	14.5	2013/08/18	medium	
K00492.01	14.2	2013/07/24	high	
K00494.01	14.6	2013/08/22	medium	
K00496.01	14.1	2013/08/13	medium	
K00499.01	14.0	2013/07/25	low	
K00500.01	14.4	2013/08/21	medium	
K00501.01	14.4	2013/07/24	medium	
K00503.01	14.5	2013/08/22	low	
K00504.01	14.3	2013/07/25	low	
K00505.01	13.9	2013/07/29	medium	
K00507.01	14.6	2013/08/22	medium	yes
K00512.01	14.6	2013/08/22	low	
K00518.01	14.0	2013/08/15	low	
K00521.01	14.5	2013/08/14	medium	yes
K00525.01	14.3	2013/07/24	medium	
K00526.01	14.2	2013/08/14	medium	
K00535.01	14.2	2013/08/13	medium	
K00536.01	14.3	2013/08/15	medium	
K00538.01	14.4	2013/08/15	medium	
K00554.01	14.4	2013/08/13	medium	
K00558.01	14.6	2013/08/22	low	yes
K00563.01	14.3	2013/07/27	high	
K00577.01	14.1	2013/07/29	medium	
K00584.01	13.9	2012/08/05	medium	yes
K00586.01	14.4	2013/07/29	medium	
K00587.01	14.3	2013/07/27	high	
K00588.01	14.0	2013/07/28	low	
K00592.01	14.1	2013/08/14	high	yes
K00607.01	14.2	2013/08/13	medium	
K00610.01	14.1	2013/08/21	medium	
K00614.01	14.3	2013/07/29	low	yes
K00617.01	14.4	2013/07/28	low	
K00618.01	14.7	2013/10/22	low	
K00641.01	13.1	2013/07/24	high	yes
K00645.01	13.5	2013/07/25	medium	yes
K00652.01	13.3	2013/07/28	high	yes
K00670.01	13.6	2013/08/13	high	
K00672.01	13.8	2013/08/14	medium	
K00678.01	13.0	2013/07/29	medium	
K00683.01	13.5	2013/07/25	medium	
K00693.01	13.8	2013/08/13	low	
K00697.01	13.5	2013/08/15	high	yes
K00728.01	15.2	2013/10/23	low	
K00730.01	15.1	2013/08/21	low	yes
K00735.01	15.3	2013/10/23	low	
K00751.01	15.6	2013/08/22	low	
K00753.01	15.2	2013/10/22	low	
K00758.01	15.0	2013/10/22	low	
K00762.01	15.2	2013/08/21	low	
K00767.01	14.8	2013/08/22	low	
K00785.01	15.3	2013/10/23	low	
K00790.01	15.1	2013/10/23	low	
K00794.01	14.8	2013/08/21	low	
K00795.01	15.4	2013/08/22	low	
K00797.01	15.5	2013/08/22	low	
K00801.01	14.8	2013/10/25	medium	yes
K00813.01	15.5	2013/08/22	low	yes
K00821.01	15.3	2013/10/23	low	
K00822.01	15.6	2013/08/22	low	
K00823.01	15.0	2013/10/23	low	
K00824.01	16.1	2013/08/21	low	
K00825.01	14.9	2013/08/22	low	
K00844.01	15.3	2013/08/22	low	
K00846.01	15.3	2013/08/22	low	
K00851.01	15.1	2013/08/17	low	
K00875.01	15.2	2013/08/22	low	
K00878.01	15.0	2013/08/22	low	
K00883.01	15.4	2013/10/23	low	
K00895.01	15.1	2013/10/23	low	
K00897.01	15.0	2013/08/18	low	
K00908.01	14.8	2013/08/21	low	
K00922.01	15.1	2013/08/21	low	
K00931.01	15.1	2013/10/23	low	yes
K00940.01	14.2	2013/07/27	medium	
K00941.01	15.1	2013/10/22	low	

Table 5 — *Continued*

KOI	m_i/mags	ObsID	Obs. qual.*	Companion?
K00945.01	14.9	2013/08/22	low	
K00969.01		2013/07/28	high	
K00972.01	9.4	2013/07/21	low	
K00974.01	9.5	2013/07/29	high	
K00976.01		2012/08/03	high (i'-band)	yes
K00981.01	10.5	2013/07/28	high	
K00992.01	15.0	2013/08/18	low	
K00993.01	14.0	2013/07/25	medium	
K00994.01	14.4	2013/07/25	medium	
K00998.01	15.5	2013/08/18	low	
K00999.01	15.1	2013/08/18	low	yes
K01007.01	15.0	2013/08/18	low	
K01014.01	15.4	2013/08/21	low	
K01022.01	15.5	2013/08/18	low	
K01024.01	14.0	2013/07/27	high	
K01029.01	14.5	2013/08/18	medium	
K01030.01	15.2	2013/08/21	low	
K01031.01	14.9	2013/08/18	low	
K01059.01	14.6	2013/08/22	medium	
K01061.01	14.3	2013/08/20	low	yes
K01066.01	15.4	2013/08/21	low	yes
K01067.01	14.5	2013/10/23	medium	yes
K01083.01	15.1	2013/08/22	low	
K01086.01	14.4	2013/08/14	low	
K01094.01	15.5	2013/08/18	low	
K01099.01	15.2	2013/08/22	low	
K01101.01	15.4	2013/08/21	low	
K01103.01	14.8	2013/08/18	low	
K01106.01	14.6	2013/08/22	medium	
K01108.01	14.4	2013/07/24	medium	
K01109.01	14.5	2013/08/22	low	
K01110.01	14.6	2013/08/21	low	
K01112.01	14.4	2013/07/27	medium	yes
K01117.01	12.7	2013/07/24	medium	
K01159.01	15.0	2013/08/22	low	
K01174.01	13.0	2013/07/29	medium	
K01187.01	14.3	2013/07/29	medium	
K01192.01	14.0	2013/07/29	low	
K01199.01	14.5	2013/10/23	low	
K01205.01	14.3	2013/07/24	medium	
K01206.01	13.4	2013/07/28	medium	
K01209.01	14.9	2013/08/21	low	
K01210.01	14.2	2013/07/28	medium	
K01214.01	14.4	2013/07/24	medium	yes
K01219.01	14.2	2013/07/29	low	
K01226.01	15.0	2013/10/23	low	
K01238.01	14.3	2013/07/25	medium	
K01245.01	14.1	2013/08/13	medium	
K01281.01	14.2	2013/08/15	low	
K01300.01	13.9	2013/08/16	medium	yes
K01302.01	14.6	2013/08/21	medium	
K01304.01	15.6	2013/10/23	low	
K01310.01	14.4	2013/08/15	medium	
K01311.01	13.3	2013/08/14	medium	
K01323.01	15.3	2013/08/18	low	
K01325.01	14.9	2013/08/21	low	
K01328.01	15.4	2013/08/21	low	
K01329.01	14.8	2013/08/22	low	
K01331.01	14.9	2013/10/23	low	
K01339.01	14.6	2013/08/18	medium	
K01341.01	14.8	2013/08/22	medium	
K01355.01	15.7	2013/08/22	low	
K01357.01	15.3	2013/08/18	low	yes
K01362.01	15.1	2013/08/21	low	
K01370.01	14.7	2013/08/22	low	
K01372.01	15.2	2013/10/23	low	
K01391.01	14.2	2013/08/13	medium	
K01397.01	14.8	2013/08/21	low	yes
K01406.01	14.5	2013/08/15	low	
K01413.01	14.2	2013/08/14	medium	
K01425.01	15.1	2013/10/23	low	
K01428.01	14.3	2013/08/17	medium	
K01431.01	13.2	2013/08/17	medium	
K01445.01	12.2	2013/08/14	high	
K01458.01	15.5	2013/10/22	low	

Table 5 — *Continued*

KOI	m_i/mags	ObsID	Obs. qual.*	Companion?
K01465.01	14.1	2013/08/17	medium	
K01470.01	15.5	2013/10/22	low	
K01474.01	12.9	2013/08/16	high	
K01475.01	15.4	2013/08/22	low	
K01491.01	15.0	2013/08/22	low	
K01495.01	15.2	2013/08/22	low	yes
K01499.01	14.2	2013/07/25	medium	
K01516.01	14.7	2013/10/23	low	
K01518.01	15.0	2013/08/22	low	
K01520.01	14.3	2013/08/16	medium	
K01522.01	14.0	2013/08/15	high	
K01527.01	14.6	2013/10/23	medium	
K01531.01	12.9	2013/08/16	medium	yes
K01532.01	12.7	2013/08/17	medium	
K01533.01	13.8	2013/08/13	low	
K01534.01	13.3	2013/07/29	medium	
K01546.01	14.2	2013/08/19	low	yes
K01549.01	14.9	2013/08/21	low	
K01552.01	15.5	2013/08/21	low	
K01553.01	15.0	2013/08/18	low	
K01573.01	14.2	2013/07/25	medium	yes
K01574.01	14.4	2013/07/28	low	
K01585.01	15.2	2013/08/22	medium	
K01586.01	14.6	2013/10/23	low	
K01591.01	15.1	2013/08/22	low	
K01599.01	14.6	2013/08/18	low	yes
K01601.01	14.4	2013/07/29	low	
K01602.01	14.7	2013/08/21	low	
K01603.01	14.3	2013/07/25	medium	
K01626.01	15.1	2013/08/21	low	
K01637.01	15.8	2013/08/21	low	
K01639.01	13.4	2013/07/28	high	
K01641.01	14.8	2013/08/21	low	
K01643.01	14.5	2013/08/22	medium	
K01646.01	14.0	2013/07/28	high	
K01648.01	14.1	2013/08/14	medium	
K01683.01	14.4	2013/08/13	medium	
K01686.01	15.1	2013/08/18	low	
K01688.01	14.3	2013/07/25	medium	
K01700.01	14.1	2013/07/27	medium	yes
K01702.01	14.9	2013/08/22	low	
K01704.01	14.6	2013/08/21	low	
K01707.01	15.1	2013/08/22	low	
K01717.01	14.3	2013/10/25	low	yes
K01731.01	15.3	2013/08/17	low	
K01733.01	15.5	2013/08/19	low	
K01746.01	14.7	2013/08/21	low	
K01760.01	15.1	2013/08/22	low	
K01762.01	14.8	2013/08/22	low	
K01784.01	13.4	2013/07/28	high	yes
K01786.01	14.2	2013/08/18	medium	
K01788.01	14.1	2013/07/25	medium	
K01793.01	15.1	2013/08/18	low	
K01797.01	12.6	2013/08/14	high	
K01798.01	14.2	2013/08/13	medium	yes
K01800.01	12.2	2013/08/15	medium	
K01801.01	14.4	2013/08/13	medium	
K01808.01	12.3	2013/07/29	high	
K01809.01	12.5	2013/08/13	medium	
K01815.01	13.5	2013/07/24	high	
K01826.01	13.2	2013/07/25	medium	
K01828.01	14.2	2013/08/13	medium	
K01829.01	15.6	2013/10/23	low	
K01830.01	14.2	2013/07/27	medium	yes
K01833.01	13.8	2013/08/17	medium	
K01837.01	13.5	2013/08/18	medium	
K01838.01	14.4	2013/08/21	medium	
K01841.01	12.9	2013/08/17	medium	
K01842.01	14.1	2013/07/24	medium	
K01848.01	13.3	2013/08/13	medium	
K01849.01	14.3	2013/08/19	low	
K01851.01	14.6	2013/08/21	medium	
K01853.01	13.3	2013/08/14	medium	yes
K01861.01	13.8	2013/07/28	high	yes
K01864.01	13.2	2013/07/24	high	

Table 5 — *Continued*

KOI	m_i/mags	ObsID	Obs. qual.*	Companion?
K01870.01	14.1	2013/07/24	medium	
K01875.01	14.3	2013/07/28	medium	
K01876.01	14.7	2013/10/22	low	
K01877.01	13.1	2013/08/14	medium	
K01881.01	14.6	2013/08/18	low	
K01885.01	14.2	2013/08/13	medium	
K01898.01	13.1	2012/08/29	medium (i'-band)	
K01899.01	14.4	2013/07/27	high	yes
K01902.01	14.0	2013/08/22	medium	
K01904.01	13.1	2013/07/27	high	
K01906.01	14.6	2013/10/22	low	
K01911.01	14.9	2013/08/22	low	
K01914.01	14.1	2013/07/29	medium	
K01920.01	14.4	2013/08/13	low	
K01928.01	13.4	2012/08/29	low (i'-band)	
K01934.01	14.2	2013/07/27	medium	
K01935.01	15.6	2013/08/17	low	
K01937.01	13.1	2013/08/14	high	
K01942.01	15.1	2013/08/21	low	
K01946.01	14.3	2013/08/15	low	
K01950.01	15.7	2013/08/22	low	yes
K01958.01	15.0	2013/07/21	medium	
K01965.01	14.1	2013/08/17	medium	
K01967.01	14.0	2013/07/29	medium	
K01969.01	14.8	2013/08/21	low	
K01972.01	13.6	2013/08/15	medium	yes
K01976.01	14.8	2013/08/21	low	
K01978.01	15.0	2012/09/13	low	
K01980.01	13.6	2013/08/15	high	
K01985.01	13.4	2013/07/24	medium	yes
K01986.01	14.5	2013/08/21	low	
K01989.01	13.1	2013/08/14	low	yes
K01990.01	14.3	2013/08/16	medium	
K01992.01	14.3	2013/08/17	medium	
K02005.01	14.4	2013/08/22	low	
K02007.01	13.0	2013/08/15	medium	
K02014.01	15.4	2013/10/23	low	yes
K02018.01	14.3	2013/07/24	medium	
K02019.01	15.4	2013/08/22	low	yes
K02023.01	14.9	2013/08/21	low	
K02024.01	14.4	2013/07/27	medium	
K02031.01	14.3	2013/08/21	medium	
K02032.01	12.0	2013/07/28	high	yes
K02034.01	15.3	2013/08/22	low	
K02036.01	15.2	2013/08/22	low	
K02039.01	14.1	2013/08/14	medium	
K02043.01	13.9	2013/07/28	high	
K02052.01	15.2	2013/08/18	low	
K02055.01	14.3	2013/07/25	low	yes
K02056.01	14.3	2013/08/16	medium	yes
K02064.01	14.8	2013/08/21	low	
K02066.01	14.7	2013/08/22	low	
K02067.01	12.3	2013/07/24	high	yes
K02069.01	13.6	2013/08/14	medium	yes
K02075.01	12.1	2013/08/17	high	
K02081.01	13.1	2013/07/27	high	
K02083.01	13.4	2013/07/28	medium	yes
K02084.01	14.8	2013/08/22	low	
K02095.01	14.5	2013/08/21	medium	
K02096.01	14.9	2013/08/19	low	yes
K02097.01	14.5	2013/07/28	low	
K02098.01	13.7	2013/07/27	medium	yes
K02099.01	14.8	2013/08/22	low	
K02100.01	14.4	2013/07/28	medium	yes
K02102.01	14.9	2013/08/22	low	
K02109.01	13.9	2013/08/17	high	
K02114.01	14.7	2013/08/22	low	
K02115.01	15.8	2013/07/21	low	yes
K02120.01	13.4	2013/07/25	high	
K02122.01	14.1	2013/07/28	medium	
K02123.01	14.2	2013/07/24	medium	
K02124.01	13.8	2013/08/15	medium	
K02130.01	15.1	2013/08/18	low	
K02131.01	14.5	2013/07/29	low	
K02132.01	14.3	2013/07/28	medium	

Table 5 — *Continued*

KOI	m_i/mags	ObsID	Obs. qual.*	Companion?
K02144.01	14.7	2013/08/21	low	
K02145.01	14.8	2013/08/22	low	
K02147.01	14.3	2013/08/16	medium	
K02148.01	13.1	2013/07/27	medium	
K02153.01	13.5	2013/07/27	low	
K02156.01	15.3	2013/08/18	low	yes
K02160.01	14.7	2013/10/23	low	
K02168.01	14.7	2013/10/22	low	
K02172.01	14.9	2013/08/22	low	
K02174.01	15.2	2012/08/07	low	yes
K02181.01	14.1	2013/07/25	medium	
K02185.01	14.2	2013/08/14	medium	
K02186.01	15.2	2013/08/18	low	
K02189.01	14.9	2013/08/21	low	
K02208.01	12.4	2013/08/16	high	
K02209.01	14.1	2013/08/13	medium	
K02218.01	14.3	2013/08/18	low	
K02225.01	14.0	2013/08/14	medium	
K02226.01	15.1	2013/08/22	low	
K02232.01	15.1	2013/08/22	low	
K02241.01	15.1	2013/08/18	low	
K02243.01	14.6	2013/08/22	low	
K02247.01	15.0	2013/07/27	medium	yes
K02253.01	14.4	2013/08/13	medium	
K02256.01	15.3	2013/08/21	low	
K02259.01	15.1	2013/08/21	low	
K02261.01	13.8	2013/07/28	high	
K02263.01	14.3	2013/08/14	medium	
K02264.01	14.2	2013/08/17	medium	
K02266.01	15.6	2013/08/22	low	
K02269.01	15.0	2013/08/22	low	
K02278.01	13.6	2013/07/28	high	
K02280.01	15.7	2013/08/18	low	
K02282.01	14.0	2013/07/24	medium	
K02286.01	14.8	2013/08/21	low	
K02288.01	15.2	2013/08/22	low	
K02290.01	14.2	2013/08/15	medium	
K02293.01	14.6	2013/08/22	medium	
K02295.01	11.4	2013/07/29	high	yes
K02296.01	14.4	2013/08/18	medium	
K02297.01	14.1	2013/07/25	low	
K02298.01	13.5	2013/08/16	high	yes
K02299.01	15.1	2013/10/23	low	
K02304.01	15.1	2013/10/23	low	
K02305.01	15.5	2013/10/23	low	
K02306.01	14.2	2013/08/22	low	
K02310.01	14.4	2013/08/15	medium	
K02311.01	12.4	2013/07/29	high	
K02314.01	14.4	2013/07/27	medium	yes
K02315.01	15.3	2013/08/22	low	
K02317.01	14.1	2013/07/27	high	yes
K02318.01	14.1	2013/08/17	medium	
K02321.01	14.5	2013/08/22	medium	
K02325.01	14.1	2013/08/13	medium	
K02333.01	13.5	2012/08/31	low (i'-band)	
K02337.01	15.6	2013/08/22	low	
K02343.01	14.2	2013/08/14	medium	
K02344.01	15.3	2013/10/23	low	
K02351.01	14.7	2013/08/18	low	
K02354.01	14.3	2013/07/27	high	
K02356.01	14.3	2013/08/15	medium	
K02363.01	14.1	2013/07/24	medium	yes†
K02371.01	14.8	2013/10/22	low	
K02373.01	14.5	2013/08/16	medium	
K02377.01	14.5	2013/07/24	medium	yes
K02378.01	14.2	2013/07/29	low	
K02380.01	14.0	2013/07/24	high	yes
K02386.01	14.7	2013/08/22	low	
K02392.01	14.8	2013/08/22	low	
K02393.01	14.6	2013/10/23	low	
K02400.01	15.4	2013/08/21	low	
K02402.01	14.2	2013/08/13	low	
K02403.01	12.7	2013/07/24	high	
K02411.01	15.2	2013/08/21	low	
K02415.01	15.5	2013/08/20	low	

Table 5 — *Continued*

KOI	m_i/mags	ObsID	Obs. qual.*	Companion?
K02417.01	15.9	2012/07/17	low	
K02418.01	15.0	2013/08/22	low	
K02419.01	15.1	2013/08/21	low	
K02421.01	14.0	2013/07/25	low	yes
K02422.01	14.5	2013/10/23	medium	
K02423.01	14.5	2013/08/22	low	
K02430.01	14.1	2013/07/28	high	
K02437.01	14.5	2013/08/21	low	
K02444.01	15.5	2013/08/21	low	
K02448.01	15.1	2013/08/22	low	
K02462.01	11.7	2013/07/24	high	
K02467.01	14.4	2013/08/16	medium	
K02468.01	15.2	2013/10/22	low	
K02469.01	14.7	2013/08/18	low	yes
K02471.01	14.3	2013/07/29	low	
K02474.01	13.9	2013/08/13	medium	yes
K02483.01	14.3	2013/07/25	medium	
K02489.01	15.5	2013/08/18	low	
K02490.01	15.4	2013/08/22	low	
K02492.01	13.7	2013/08/17	high	
K02493.01	15.0	2013/08/22	low	yes
K02504.01	15.7	2013/10/23	low	
K02507.01	15.7	2013/10/23	low	
K02508.01	14.9	2013/08/21	low	
K02516.01	13.1	2013/07/27	high	yes
K02517.01	14.3	2013/07/29	low	
K02519.01	14.0	2013/08/13	medium	
K02523.01	15.6	2013/08/21	low	
K02529.01	15.4	2013/08/18	low	
K02531.01	15.1	2013/08/22	low	
K02536.01	14.2	2013/07/24	low	
K02542.01	14.8	2013/08/21	low	yes
K02550.01	15.2	2013/08/22	low	
K02551.01	15.5	2013/10/23	low	yes
K02552.01	14.3	2013/08/13	medium	
K02560.01	15.1	2013/08/22	low	
K02569.01	14.0	2013/07/27	high	
K02571.01	14.2	2013/08/13	medium	
K02573.01	15.6	2013/08/21	low	
K02577.01	13.4	2013/08/17	medium	
K02587.01	14.9	2013/10/23	low	
K02590.01	11.5	2013/08/16	high	
K02598.01	14.0	2013/08/13	medium	yes
K02601.01	13.8	2013/08/13	high	yes
K02607.01	14.3	2013/07/29	medium	
K02620.01	15.6	2013/10/22	low	
K02623.01	13.3	2013/08/17	medium	
K02626.01	15.2	2013/10/25	low	
K02627.01	14.4	2013/07/29	low	
K02634.01	15.7	2013/08/21	low	
K02635.01	12.7	2013/07/24	high	
K02636.01	12.1	2013/08/14	high	
K02649.01	14.4	2013/07/28	medium	
K02652.01	14.7	2013/08/18	low	
K02654.01	15.6	2013/10/22	low	
K02656.01	14.9	2013/10/23	low	
K02658.01	14.2	2013/08/14	medium	
K02659.01	12.7	2013/08/13	medium	
K02664.01	15.3	2013/08/18	low	yes
K02666.01	15.1	2013/08/22	low	
K02672.01	11.7	2013/08/14	high	
K02674.01	13.2	2013/07/27	high	
K02675.01	12.2	2013/07/28	high	
K02677.01	13.3	2013/08/13	high	
K02678.01	11.6	2013/08/13	high	
K02679.01	13.3	2013/07/25	high	yes
K02680.01	14.4	2013/07/24	medium	
K02681.01	15.7	2013/10/23	low	yes
K02686.01	13.5	2013/07/25	medium	
K02687.01	10.0	2013/08/13	high	
K02690.01	13.2	2013/07/28	high	
K02693.01	12.8	2013/07/29	high	
K02696.01	12.9	2013/08/14	high	
K02698.01	13.8	2013/07/24	high	
K02700.01	14.9	2013/08/22	low	

Table 5 — *Continued*

KOI	m_i/mags	ObsID	Obs. qual.*	Companion?
K02704.01	17.0	2013/08/21	low	
K02705.01	14.3	2013/07/25	high	yes
K02706.01	10.2	2013/08/14	high	
K02707.01	14.2	2013/07/24	medium	yes
K02711.01	13.5	2013/07/29	medium	yes
K02712.01	11.0	2013/07/29	high	
K02714.01	13.2	2013/08/18	high	
K02717.01	12.3	2013/08/14	high	
K02720.01	10.2	2013/07/29	high	
K02722.01	13.2	2013/08/14	high	yes
K02723.01	14.3	2013/07/27	medium	
K02729.01	13.7	2013/08/18	medium	yes
K02730.01	13.7	2013/07/28	high	
K02732.01	12.7	2013/08/15	high	
K02733.01	13.6	2013/08/13	high	
K02734.01	15.5	2013/08/21	low	
K02743.01	13.5	2013/08/14	high	yes
K02748.01	13.8	2013/07/29	low	
K02750.01	15.7	2013/08/18	low	
K02753.01	13.4	2013/07/27	high	
K02754.01		2013/08/14	high	yes
K02755.01	12.0	2013/07/28	high	
K02756.01	14.6	2013/10/23	medium	
K02757.01	14.4	2013/08/13	low	
K02759.01	14.0	2013/08/18	medium	
K02771.01		2013/08/16	high	yes
K02775.01	14.7	2013/08/22	low	
K02778.01	15.1	2013/08/22	low	
K02779.01	14.8	2013/10/22	low	yes
K02785.01	13.9	2013/08/16	high	
K02786.01	13.7	2013/08/15	medium	
K02789.01	14.3	2013/08/14	medium	
K02790.01	13.1	2013/07/24	high	
K02795.01	15.1	2013/08/17	low	
K02798.01	13.6	2013/07/29	medium	
K02801.01	10.6	2013/07/24	high	
K02803.01	12.1	2013/08/13	high	yes
K02805.01	13.2	2013/08/17	high	
K02807.01	13.7	2013/07/28	high	yes
K02812.01	14.2	2013/07/27	high	yes
K02822.01	15.2	2013/08/18	low	
K02827.01	14.3	2013/08/13	low	
K02829.01	12.7	2013/08/14	high	
K02830.01	13.8	2013/07/24	high	
K02833.01	12.4	2013/07/27	high	
K02836.01	14.9	2013/10/22	low	yes
K02837.01	13.1	2013/08/15	high	yes
K02838.01	13.2	2013/08/13	high	yes
K02840.01	13.7	2013/07/25	high	
K02842.01	15.5	2013/07/27	high	
K02848.01	12.3	2013/08/14	high	yes
K02849.01	14.3	2013/08/16	medium	
K02855.01	14.2	2013/08/13	medium	
K02857.01	13.5	2013/07/27	medium	
K02859.01	13.6	2013/08/16	high	yes
K02866.01	14.0	2013/07/27	medium	
K02867.01	12.6	2013/08/14	high	
K02869.01	13.6	2013/07/27	high	
K02882.01	15.0	2013/08/21	low	
K02883.01	15.4	2013/08/22	low	
K02890.01	15.0	2013/08/22	low	
K02904.01	12.5	2013/07/24	low	yes
K02906.01	13.6	2013/07/25	high	
K02910.01	15.0	2013/08/19	low	yes
K02913.01	12.7	2013/07/29	high	
K02914.01	12.1	2013/07/24	high	yes
K02915.01		2013/07/29	medium	
K02923.01	14.4	2013/08/13	low	
K02924.01	14.3	2013/08/13	medium	
K02935.01	13.5	2013/07/24	high	
K02936.01	14.2	2013/07/27	high	
K02942.01	15.2	2013/08/18	low	
K02943.01	13.7	2013/08/13	high	
K02948.01	11.7	2013/08/14	high	
K02949.01	13.1	2013/07/29	medium	yes

Table 5 — *Continued*

KOI	m_i/mags	ObsID	Obs. qual.*	Companion?
K02951.01	13.2	2013/07/25	low	
K02956.01	11.7	2013/07/28	high	
K02959.01	15.3	2013/08/22	low	
K02961.01	12.4	2013/08/16	high	
K02962.01	14.0	2013/07/25	low	yes
K02963.01	14.4	2013/08/13	medium	
K02964.01	13.9	2013/07/24	medium	
K02967.01	15.3	2013/08/22	low	
K02968.01		2013/08/15	high	
K02970.01	12.7	2013/07/28	high	
K02971.01	12.6	2013/07/24	high	yes
K02977.01	13.6	2013/08/15	high	
K02982.01	14.0	2013/08/15	medium	
K02984.01	12.9	2013/07/24	high	yes
K02989.01	15.1	2013/08/18	low	
K02992.01	15.4	2013/10/23	low	
K02994.01	14.4	2013/08/16	medium	
K02998.01	15.6	2013/08/21	low	
K03004.01	14.7	2013/08/21	medium	
K03007.01	14.3	2013/08/14	low	
K03008.01	11.9	2013/07/27	high	
K03015.01	13.1	2013/08/16	high	
K03017.01	13.1	2013/08/15	high	
K03019.01	14.7	2013/10/22	low	
K03026.01	14.6	2013/08/22	medium	
K03029.01	14.7	2013/08/18	low	yes
K03038.01	14.0	2013/07/25	medium	
K03039.01	13.7	2013/07/29	high	
K03041.01	14.0	2013/07/25	medium	yes
K03048.01	14.4	2013/08/14	medium	
K03050.01	15.1	2013/08/18	low	
K03052.01	13.3	2013/07/29	medium	
K03053.01	15.5	2013/08/21	low	
K03056.01	15.6	2013/10/23	low	
K03057.01	15.6	2013/08/22	low	
K03060.01	12.7	2013/08/16	high	
K03061.01	14.0	2013/07/25	medium	
K03065.01	14.4	2013/07/24	medium	
K03068.01	14.7	2013/08/18	medium	
K03069.01	14.7	2013/08/19	low	yes
K03071.01	14.1	2013/08/13	medium	
K03073.01	14.2	2013/08/14	medium	yes
K03075.01	12.9	2013/07/28	high	
K03083.01	12.7	2013/08/13	high	
K03086.01	15.4	2013/08/22	low	
K03093.01	13.4	2013/07/29	medium	
K03097.01	11.8	2013/07/24	high	
K03105.01	15.0	2013/10/23	low	
K03109.01	13.5	2013/07/29	medium	
K03117.01	12.9	2013/08/13	high	
K03119.01	16.2	2013/08/22	low	
K03122.01	12.0	2013/08/15	high	
K03123.01	14.8	2013/08/19	low	
K03125.01	12.8	2013/08/15	high	
K03127.01	14.7	2013/08/22	low	
K03128.01	13.2	2013/08/13	high	
K03130.01	13.5	2013/07/24	medium	
K03140.01	15.0	2013/08/22	low	
K03142.01	15.1	2013/08/22	low	
K03145.01	15.3	2013/08/18	low	
K03146.01	13.9	2013/08/15	medium	
K03147.01	14.1	2013/07/29	low	
K03158.01		2013/07/21	high	yes
K03179.01	10.5	2013/07/24	high	
K03184.01		2013/08/13	high	
K03190.01	11.1	2013/07/27	high	yes
K03194.01	11.4	2013/08/17	high	
K03196.01	11.4	2013/07/28	high	
K03203.01	11.7	2013/07/24	high	
K03204.01		2013/08/16	high	
K03208.01	11.8	2013/07/29	high	
K03209.01	11.8	2013/08/13	high	
K03220.01	12.0	2013/08/17	high	
K03232.01	12.1	2013/07/27	high	
K03234.01	12.2	2013/08/14	high	

Table 5 — *Continued*

KOI	m_i/mags	ObsID	Obs. qual.*	Companion?
K03236.01	12.2	2013/07/27	high	
K03237.01	12.1	2013/07/28	high	
K03242.01	12.4	2013/07/28	high	
K03245.01	12.3	2013/07/25	high	yes
K03246.01	12.1	2013/08/16	high	
K03255.01	14.0	2013/07/27	high	yes
K03259.01	15.4	2013/08/22	low	
K03260.01	14.5	2013/08/18	low	
K03261.01	14.2	2013/08/17	medium	
K03277.01	12.9	2013/07/24	high	yes
K03278.01	14.5	2013/08/22	medium	
K03284.01	13.8	2013/08/22	low	yes
K03288.01	14.0	2013/07/24	high	yes
K03296.01	14.2	2013/07/27	high	
K03301.01	14.0	2013/08/14	medium	
K03308.01	13.9	2013/07/29	medium	
K03309.01	14.4	2013/08/17	medium	yes
K03310.01	13.3	2013/08/18	high	
K03311.01	14.0	2013/08/15	medium	
K03315.01	13.8	2013/08/15	high	
K03324.01	15.7	2013/10/23	low	yes
K03334.01	15.0	2013/08/13	high	
K03339.01	14.4	2013/10/22	low	yes
K03340.01	13.6	2013/07/28	high	
K03343.01	14.8	2013/08/22	low	
K03345.01	14.5	2013/08/15	medium	
K03346.01	13.2	2013/07/28	high	
K03353.01	14.3	2013/07/24	low	
K03363.01	13.6	2013/08/17	high	
K03365.01	14.2	2013/08/17	medium	
K03371.01	13.5	2013/08/17	high	
K03374.01	14.3	2013/07/27	high	
K03377.01	14.9	2013/08/22	low	yes
K03379.01	15.1	2013/08/22	low	
K03384.01	13.0	2013/07/27	high	
K03385.01	15.0	2013/08/21	low	
K03389.01	14.4	2013/07/29	low	
K03398.01	13.4	2013/07/24	high	
K03401.01	14.2	2013/07/28	medium	yes
K03403.01	12.9	2013/08/17	high	
K03408.01	14.6	2013/10/23	medium	
K03414.01	14.9	2013/08/22	low	
K03419.01	12.9	2013/07/29	medium	
K03423.01	14.1	2013/07/28	medium	
K03425.01	13.0	2013/07/24	high	
K03429.01	15.1	2013/10/23	low	
K03430.01	15.4	2013/10/23	low	
K03437.01	14.4	2013/08/13	medium	
K03438.01	13.6	2013/08/14	high	
K03439.01	14.0	2013/07/24	medium	yes
K03440.01	15.4	2013/08/18	low	
K03444.01	13.0	2013/07/25	high	yes
K03448.01	14.7	2013/08/22	low	
K03451.01	13.9	2013/08/17	medium	
K03456.01	12.8	2013/08/13	high	
K03459.01	15.0	2013/08/21	low	yes
K03460.01	14.3	2013/07/27	high	yes
K03468.01	14.1	2013/07/24	medium	yes
K03474.01	14.0	2013/07/24	medium	
K03481.01	14.3	2013/08/15	medium	
K03484.01	15.0	2013/08/21	low	
K03486.01	14.1	2013/07/24	medium	yes
K03496.01	13.8	2013/08/14	high	
K03497.01	13.0	2013/10/24	medium	yes
K03500.01	13.0	2013/07/25	high	yes
K03503.01	13.7	2013/07/29	medium	
K03506.01	12.8	2013/07/24	high	
K03528.01	12.6	2013/07/29	high	
K03541.01	13.6	2013/07/28	high	
K03557.01	13.2	2013/07/29	high	
K03573.01	13.5	2013/08/16	high	
K03583.01	12.5	2013/07/24	high	
K03602.01	13.7	2013/08/14	medium	
K03608.01	13.4	2013/08/14	high	
K03627.01	15.0	2013/08/22	low	

Table 5 — *Continued*

KOI	m_i/mags	ObsID	Obs. qual.*	Companion?
K03663.01	12.4	2013/08/18	high	
K03680.01	14.3	2013/08/14	low	
K03681.01		2013/07/24	high	
K03683.01	11.9	2013/08/17	high	
K03689.01	13.9	2013/08/13	low	
K03721.01	13.9	2013/07/29	medium	
K03728.01	12.2	2013/08/15	high	
K03762.01	14.6	2013/10/23	low	
K03780.01	13.9	2013/08/14	medium	
K03782.01	13.2	2013/08/16	high	
K03787.01	13.7	2013/08/14	high	
K03811.01	13.7	2013/07/28	high	
K03835.01	12.5	2013/07/24	high	
K03837.01	14.0	2013/08/15	medium	
K03848.01	14.0	2013/08/18	medium	
K03864.01	12.6	2013/07/28	high	
K03875.01	13.3	2013/08/17	high	
K03876.01	12.4	2013/07/29	high	
K03891.01	13.4	2013/07/27	high	yes
K03892.01	12.5	2013/08/17	high	
K03893.01	15.2	2013/08/21	low	
K03907.01	12.5	2013/07/27	high	yes
K03908.01	11.9	2013/07/24	high	
K03911.01	14.3	2013/08/15	medium	
K03916.01	15.0	2013/08/18	low	
K03925.01	13.8	2013/08/18	medium	
K03935.01	14.6	2013/08/22	medium	
K03943.01	12.5	2013/08/15	high	
K03946.01	13.1	2013/08/13	high	yes
K03966.01	14.0	2013/07/29	low	
K03984.01	14.2	2013/07/29	medium	
K03991.01	12.9	2013/08/13	high	
K04004.01	12.5	2013/07/27	high	yes
K04005.01	14.3	2013/07/24	low	
K04014.01	13.5	2013/08/16	high	
K04016.01	13.6	2013/07/27	medium	
K04021.01	12.5	2013/08/16	high	yes
K04032.01	12.4	2013/07/28	high	
K04037.01	12.7	2013/07/24	high	
K04051.01	14.8	2013/08/21	low	
K04053.01	12.6	2013/07/25	high	yes
K04054.01	14.3	2013/07/28	medium	
K04056.01	14.1	2013/07/25	medium	
K04060.01	13.7	2013/08/14	high	
K04066.01	13.6	2013/08/15	high	
K04067.01	14.0	2013/07/29	medium	
K04068.01	15.1	2013/08/22	low	
K04069.01	14.5	2013/08/17	medium	
K04072.01	13.3	2013/07/27	high	
K04097.01	13.0	2013/07/29	high	
K04098.01	13.5	2013/08/15	low	yes
K04109.01	14.2	2013/07/27	high	
K04123.01	13.3	2013/07/25	medium	
K04129.01	13.2	2013/08/15	high	
K04136.01	13.8	2013/07/24	medium	
K04145.01	14.1	2013/07/27	medium	yes
K04146.01	13.3	2013/08/15	high	
K04149.01	14.1	2013/10/22	low	yes
K04150.01	14.5	2013/10/23	medium	
K04152.01	12.9	2013/08/14	high	
K04153.01	14.5	2013/10/23	low	
K04156.01	13.6	2013/07/28	high	
K04157.01	12.6	2013/08/13	high	
K04159.01	14.2	2013/08/13	medium	
K04160.01	13.2	2013/08/13	high	
K04166.01	15.0	2013/08/18	low	yes
K04169.01	14.4	2013/08/22	medium	
K04184.01	13.2	2013/07/24	high	
K04188.01	13.0	2013/07/27	high	
K04190.01	13.4	2013/08/18	medium	
K04194.01	15.0	2013/08/21	low	yes
K04198.01	12.5	2013/07/29	high	
K04199.01	14.0	2013/07/27	medium	
K04205.01	14.2	2013/07/28	medium	yes
K04208.01	15.3	2013/08/17	low	yes

Table 5 — *Continued*

KOI	m_i/mags	ObsID	Obs. qual.*	Companion?
K04209.01	15.7	2013/08/19	low	yes
K04212.01	13.8	2013/07/25	high	
K04215.01	13.7	2013/07/24	medium	
K04226.01	12.6	2013/07/24	high	yes
K04230.01	13.7	2013/07/24	high	
K04235.01	13.1	2013/08/17	high	
K04242.01	14.2	2013/08/15	low	
K04245.01	13.4	2013/08/18	high	
K04251.01	13.6	2013/08/14	high	
K04252.01	13.4	2013/08/17	high	
K04253.01	14.1	2013/08/13	low	
K04269.01	12.9	2013/08/13	high	
K04273.01	12.5	2013/08/14	high	
K04274.01	15.1	2013/08/22	low	yes
K04276.01	12.4	2013/07/29	high	
K04287.01	11.1	2013/08/17	high	yes
K04288.01	12.3	2013/07/29	high	
K04292.01	12.7	2013/08/15	high	yes†
K04295.01	14.8	2013/08/18	medium	
K04296.01	12.9	2013/07/25	high	
K04300.01	15.7	2013/10/23	low	
K04301.01	12.9	2013/07/27	high	
K04302.01	13.5	2013/07/28	high	
K04304.01	13.9	2013/08/16	medium	
K04312.01	13.7	2013/08/17	high	
K04313.01	14.1	2013/08/13	medium	yes
K04318.01	12.5	2013/08/14	high	
K04320.01	14.0	2013/07/29	medium	
K04325.01	15.5	2013/10/23	low	
K04327.01	14.8	2013/10/23	low	
K04329.01	11.9	2013/08/18	high	yes
K04331.01	13.0	2013/07/29	medium	yes
K04335.01	13.9	2013/08/16	high	
K04337.01	14.5	2013/10/23	medium	
K04341.01	13.1	2013/07/27	high	
K04347.01	14.6	2013/08/22	low	
K04356.01	15.5	2013/08/21	low	
K04367.01	13.8	2013/07/24	medium	
K04374.01	13.9	2013/07/28	high	
K04382.01	14.0	2013/08/14	high	
K04383.01	13.7	2013/08/16	high	
K04389.01	14.8	2013/08/21	low	yes
K04390.01	16.1	2013/08/18	low	
K04393.01	15.0	2013/08/21	low	
K04395.01	15.4	2013/08/21	low	
K04399.01	11.8	2013/07/24	high	yes
K04400.01	13.6	2013/07/24	medium	
K04403.01	15.5	2013/08/21	low	
K04407.01	11.0	2013/07/24	high	yes
K04409.01	12.3	2013/07/24	high	yes
K04411.01	13.2	2013/07/28	high	
K04423.01	13.0	2013/07/24	high	
K04427.01	15.0	2013/08/22	low	
K04428.01	14.4	2013/07/24	medium	
K04431.01	12.5	2013/08/14	high	
K04435.01	13.4	2013/07/24	high	
K04443.01	13.7	2013/08/13	high	yes
K04446.01	12.2	2013/08/15	high	
K04456.01	14.9	2013/08/18	low	
K04457.01	13.7	2013/08/17	high	
K04463.01	14.6	2013/07/27	medium	yes
K04474.01	15.6	2013/08/21	low	
K04478.01	14.3	2013/07/29	medium	
K04482.01	12.5	2013/07/24	high	
K04495.01	15.2	2013/08/22	low	yes
K04505.01	13.5	2013/07/25	high	
K04510.01	14.2	2013/08/15	medium	
K04520.01	14.0	2013/08/13	medium	
K04523.01	14.6	2013/08/21	medium	yes
K04530.01	14.0	2013/08/18	medium	
K04541.01	15.2	2013/08/22	low	
K04554.01	14.4	2013/07/28	medium	
K04556.01	11.8	2013/08/17	high	
K04558.01	14.4	2013/07/29	low	
K04561.01	14.0	2013/08/14	high	

Table 5 — *Continued*

KOI	m_i/mags	ObsID	Obs. qual.*	Companion?
K04563.01	14.3	2013/08/14	medium	
K04567.01	13.6	2013/07/24	high	yes
K04570.01	14.5	2013/07/28	medium	
K04575.01	13.0	2013/08/16	high	yes
K04580.01	12.8	2013/08/13	high	yes
K04581.01	13.4	2013/07/24	high	
K04582.01	11.6	2013/07/27	high	yes
K04586.01	14.2	2013/08/17	medium	
K04588.01	12.8	2013/08/15	medium	
K04591.01	15.0	2013/08/18	low	
K04601.01	13.6	2013/07/28	high	
K04603.01	13.5	2013/08/14	high	
K04605.01	13.3	2013/08/18	high	
K04613.01	13.7	2013/08/13	high	
K04614.01	13.7	2013/07/24	medium	
K04617.01	13.5	2013/08/16	high	
K04627.01	14.8	2013/08/18	low	
K04633.01	13.6	2013/08/14	medium	
K04634.01	13.5	2013/07/24	high	yes
K04637.01	10.3	2013/08/15	high	
K04644.01	14.8	2013/08/18	medium	
K04651.01	13.6	2013/07/25	high	yes
K04656.01	13.7	2013/07/29	medium	yes
K04657.01	13.0	2013/07/29	high	yes
K04663.01	12.5	2013/08/13	high	
K04674.01	13.4	2013/07/24	high	
K04680.01	15.3	2013/08/18	low	
K04691.01	14.3	2013/08/14	medium	
K04693.01	13.2	2013/08/13	medium	
K04699.01	12.8	2013/08/13	high	yes
K04706.01	13.5	2013/07/28	medium	
K04709.01	15.7	2013/08/21	low	
K04737.01	14.5	2013/10/23	medium	
K04744.01	13.6	2013/07/28	medium	
K04747.01	14.8	2013/08/22	low	
K04754.01	15.1	2013/08/22	low	
K04763.01	13.9	2013/07/28	high	
K04768.01	15.4	2013/10/23	low	yes
K04772.01	15.3	2013/08/18	low	
K04773.01	13.4	2013/07/27	high	
K04775.01	12.7	2013/08/14	high	
K04776.01	14.6	2013/08/21	medium	
K04782.01	15.6	2013/08/21	low	
K04792.01	14.0	2013/08/15	medium	yes
K04797.01	15.3	2013/08/22	low	yes
K04801.01	15.0	2013/10/23	low	
K04811.01	13.6	2013/08/15	medium	
K04812.01	15.5	2013/10/23	low	yes
K04813.01	13.3	2013/07/28	low	yes
K04818.01	12.9	2013/08/15	high	
K04822.01	13.3	2013/08/16	high	
K04823.01	12.5	2013/08/17	high	yes
K04826.01	14.4	2013/07/29	low	
K04829.01	14.0	2013/08/18	medium	
K04833.01	13.4	2013/08/14	high	
K04834.01	12.8	2013/08/14	high	
K04839.01	13.3	2013/07/25	medium	
K04849.01	14.0	2013/07/25	medium	
K04850.01	13.9	2013/07/25	medium	
K04852.01	14.3	2013/08/15	medium	
K04854.01	14.1	2013/08/15	medium	
K04855.01	14.4	2013/08/16	medium	
K04871.01	12.9	2013/10/25	medium	yes
K04875.01	15.2	2013/08/22	low	
K04877.01	14.3	2013/08/14	medium	
K04887.01	12.7	2013/07/28	high	
K04891.01	15.5	2013/08/22	low	
K04892.01	14.0	2013/08/15	medium	
K04907.01	13.6	2013/08/13	high	
K04914.01	14.0	2013/08/15	medium	

* All observations taken in the LP600 filter unless noted by (i'-band).

† Companion originally discovered in NIRC2 image, see Table 4.